A non-equilibrium control oriented model for the pressurizer dynamics

Alessandro Pini[a], Antonio Cammi[a,*], Luigi Colombo[a], Andrea Borio Tigliole[b,1]

[a] Politecnico di Milano Department of Energy, Via La Masa 34, 20156 Milano, Italy
[b] University of Pavia, Via Aselli 41, 27100 Pavia, Italy

This paper deals with a new Control Oriented Model (COM) aimed at studying the dynamic behaviour of the pressurizer in Pressurized Water Reactors (PWRs). In literature, most of the pressurizer COMs treat the vapour and the water filling the system as a homogeneous mixture by adopting the thermodynamic equilibrium as-sumption. This hypothesis involves a reduced set of governing equations that is suitable for the study of the pressurizer dynamics in a simplified way since interphase and non-equilibrium phenomena (e.g., water drops and vapour bubbles generation) are neglected. To overcome this limitation, an innovative COM based on the non-equilibrium approach is developed. The new model is obtained from closed-rigid system mass, energy and volume balances and allows selecting a different thermodynamic state for each phase, according to the non-equilibrium framework. In addition, while equilibrium models take into account only the heat transfer from the electrical heating of PWR pressurizers, the new COM considers also the following processes occurring in the system volume: the water drops and vapour bubbles generation (inside the vapour and liquid phase, respec-tively), the condensation on sprayed drops, the heat exchange between vapour and water and thermal losses toward the external environment. The new COM is also characterized by a multiple control volume formulation to reach a good accuracy for several transients (also the complete emptying) that can be experimented by a pressurizer. The experimental data of "loss-of-load" transients in the Shippingport reactor are used to assess the new COM. A code to code comparison is carried out using RELAP5 as reference.

Keywords: Pressurizer, Equilibrium and non-equilibrium approach, Control oriented modelling, Thermal hydraulics, RELAP5

1. Introduction

In Pressurized Water Reactors (PWRs), the cooling water of primary loop expands or contracts whenever temperature variations occur. In order to accommodate the resulting volume changes and keep the pressure of the system within prescribed limits, the pressurizer is needed. Such component is a cylindrical steel tank containing, at steady-state, saturated water in the lower region and saturated vapour in the upper one. Moreover, it is provided with:

- Electrical heaters immersed in the water to prevent pressure decrease.
- Sprayers in the upper region to contrast pressure increase.
- Relief valves on the top of the tank to counteract excessive overpressure.

Since the control of the pressure during transients is essential to operate PWRs safely and mitigate the consequence of a possible accident, the pressurizer dynamics must be carefully modelled and investigated.

Pressurizer models can be distinguished between Safety Oriented Models (SOMs) and Control Oriented models (COMs). SOMs adopt a complete description of the system based on mass, momentum and energy balances. They are able to reproduce carefully the pressurizer transients, but are not suitable to study its dynamic and control features. On the contrary, COMs employ a simplified set of governing equations (usually mass and energy balance for homogenous water vapour mixtures), which allows for a straightforward investigation of the control characteristics of the system.[2]

As for the possible modelling approaches, two different strategies can be also followed in order to describe vapour and fluid interactions: the Equilibrium Approach, usually adopted for COMs, (EA) and the Non-Equilibrium Approach (NEA), generally implemented in SOMs. Equilibrium models apply the conservation balances to the vapour and

Received 19 February 2017;
Received in revised form 21 June 2017;
Accepted 18 February 2018

* Corresponding author. Politecnico di Milano, via La Masa 34, 20156 Milano, Italy.
E-mail addresses: alessandro.pini@polimi.it (A. Pini), antonio.cammi@polimi.it (A. Cammi), luigi.colombo@polimi.it (L. Colombo), andrea.borio@unipv.it (A.B. Tigliole).

[1] Currently at the IAEA.

[2] COMs allow for low-cost real-time simulations (conversely SOMs' computational burden can be very high) and can be adopted to develop and optimize different control strategies. In this regard, COMs are usually based on block structures and permit a clear identification of inputs, outputs and state variables. A feature that is very useful to analyse the dynamic properties of a system (e.g., the linearization process can be applied with low efforts).

Published Journal Article available at: https://doi.org/10.1016/j.pnucene.2018.02.017

water as a saturated homogenous mixture. Conversely, non-equilibrium models apply the conservation equations to the water and vapour in the pressurizer separately. According to Nahavandi and Makkenchery (1970), non-equilibrium models are more realistic than the equilibrium ones.

The paper is organized as follows. Section 2 deals with the state of the art of pressurizer-dynamics modelling. In Section 3, the new COM is described. In Section 4, the mathematical formulation of the new model is presented. Section 5 illustrates the validation of the model against Shippingport experimental data (Redfield et al., 1967). Besides, a comparison between new COM results and a RELAP5 pressurizer model is presented. Section 6 presents a complete emptying out-surge test. In Section 7, the main conclusions are drawn. At the end of the paper, an Appendix provides more details about the matrix representation adopted to solve the governing equations.

2. State of the art

Regarding safety applications, the first study of the pressurizer behaviour is presented in Gajewski (1955) and adopts the thermodynamic equilibrium assumption, while the first non-equilibrium approach is proposed by Sorenson (1960). In this study, the system is divided into three rigid boundary control volumes with fixed thermodynamic state. In particular, the pressurizer is composed by an upper zone of saturated vapour, an intermediate one of saturated water and a lower one of subcooled water.

The a priori assumption concerning the thermodynamic is overcome in Redfield et al. (1967), where a single control volume coinciding with the entire pressurizer is chosen. In particular, such control volume is subdivided into two moving boundary regions (one for the vapour and one for the water) whose thermodynamic state is dynamically selected during the simulation according to the enthalpy value.

From the control analysis point of view, equilibrium COMs are presented in Szabo et al. (2010), Zhang et al. (2012) and Sungwhan and Jin (2012) for the study of different control strategies, while non-equilibrium COMs can be found in Kuridan and Beynon (1998) and Botelho et al. (2010). In the work of Kuridan and Beynon (1998), a linearized non-equilibrium model with single control volume and two moving boundary regions is developed in order to study the pressurizer dynamics of the Safety Integral Reactor (SIR). In the analysis of Botelho et al. (2010), a Multiple Control Volume (MCV) strategy is adopted. The pressurizer is divided into two fixed boundary control volumes, a lower one with a single region for subcooled water (a priori fixed thermodynamic state) and an upper one composed by two regions with moving boundary (one for the vapour and one for the water) whose thermodynamic state can vary during the simulation. Thanks to the adoption of MCVs, the axial temperature distribution inside the liquid phase can be reproduced. However, a fixed thermodynamic state region is introduced. This is a limitation that is ridden over by the new COM developed in the present work.

3. Description of the model

Hereinafter, the new COM developed in this work (based on NEA and on the selection of MCVs) is indicated with the acronyms COM-MCV. In this model, mass and energy balances are applied to each phase in all control volumes and heat and mass transfers are possible between the different zones. Moreover, the following assumption are adopted:

- Water evaporation is considered as bulk process.
- Vapour condensation is considered both as bulk and surface phenomenon.[3]
- Heat losses occur from pressurizer tank to external environment.
- The water sprayed inside the pressurizer comes from the reactor coolant cold leg (enthalpy fixed during the simulation).
- Spray and condensate mixture enters the liquid phase as saturated water.
- In-surge[4] water comes from the reactor coolant hot leg (enthalpy fixed during the simulation).
- Vapour condensation on pressurizer walls, and delay times of bubble (condensate) rise (fall) are neglected.

To completely avoid a priori assumptions about the thermodynamic state of the different regions and to take into account axial temperature distributions inside the liquid phase, the COM-MCV is composed by three sub-models (see Fig. 1):

- Two Regions Single Volume sub-model (TRSV).
- Two Regions Double Volume sub-model (TRDV).
- Two Regions Triple Volume sub-model (TRTV).

During every simulation, a global routine selects the correct sub-model by means of a thermodynamic and a water level criterion. If necessary, multiple switches are possible. The TRSV sub-model is based on the selection of a single control volume coinciding with the entire pressurizer.

A moving boundary splits this control volume into two different zones, an upper one containing only vapour and a lower one for water. Vapour and water can experiment all the possible stable thermodynamic state and not only the equilibrium one. Vapour can be saturated or superheated, whereas water can be saturated or subcooled, but no phase can exist in metastable form.

The TRDV and the TRTV sub-models are based on the selection of additional fixed boundary control volumes for the liquid zone. The water filling these control volumes is always treated as subcooled. In this way, axial temperature distributions inside the liquid region can be taken into account. On the contrary, the single volume approach can only compute a global mean temperature for the liquid phase, since it applies a zero-dimensional approximation of the region. Axial temperature distributions can arise during in-surge transients (see Section 4) and can impair the simulation if they are not considered. The three sub-models are not mutually exclusive. At the beginning of every simulation, the global routine selects the TRTV sub-model (Fig. 1c) by assuming that the moving-boundary region ③ is filled with saturated vapour and water and regions, ② and ① with subcooled water. If the subcooled liquid region ② empties or reaches the saturation condition, the TRDV is chosen (Fig. 1b). Similarly, if the subcooled liquid region ① becomes saturated or empty, the TRSV sub-model is picked (Fig. 1a). Of course, the procedure is reversible, from TRSV it is possible to switch to TRDV and then to TRTV. A conceptual flow chart is reported in Fig. 2, where L1, L2 and L3 are length related to the water level inside the pressurizer.

4. Jump conditions and governing equations

The governing equations of the COM-MCV model are represented by mass and energy balances and jump conditions. In this regard, jump conditions are balance equations for mass and energy transfer across vapour liquid interfaces. Since no mass and energy sources or sinks exist at each interface, jump conditions assert that the sum of all mass and energy transfer rates across the interface must be equal to zero.

[3] Vapour which is condensing on the pressurizer wall is evaluated by applying the Nusselt theory following Incropera and Dewitt (1996).

[4] The "in-surge" term specifies a water mass flow rate coming from the primary system into the pressurizer volume. Conversely, "out-surge" term is adopted to indicate water mass flow rate coming out by the pressurizer volume.

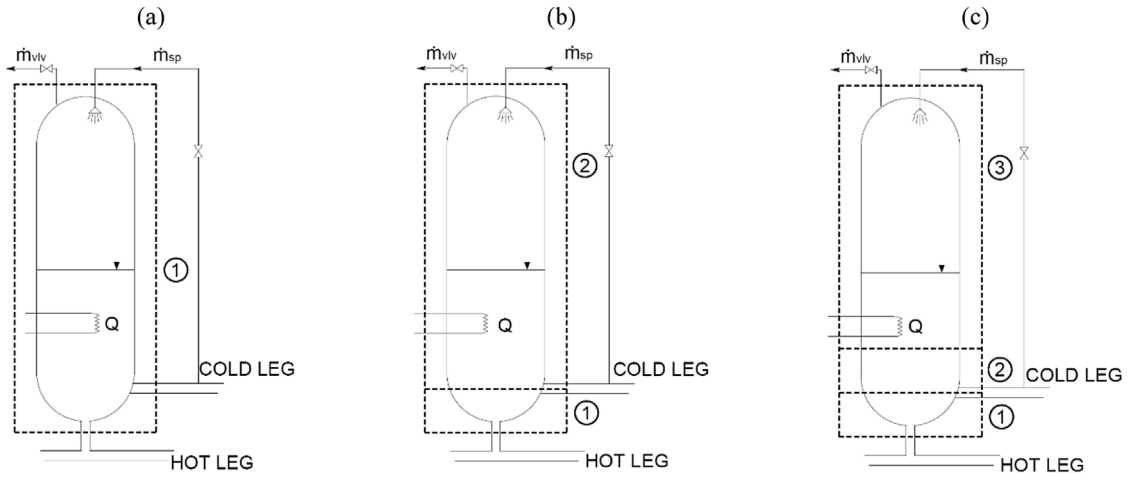

Fig. 1. Pressurizer COM-MCV sub-models, Two Regions Single Volume (TRSV) sub-model (a), Two Regions Double Volume (TRDV) sub-model (b) and Two Regions Triple Volume (TRTV) sub-model (c).

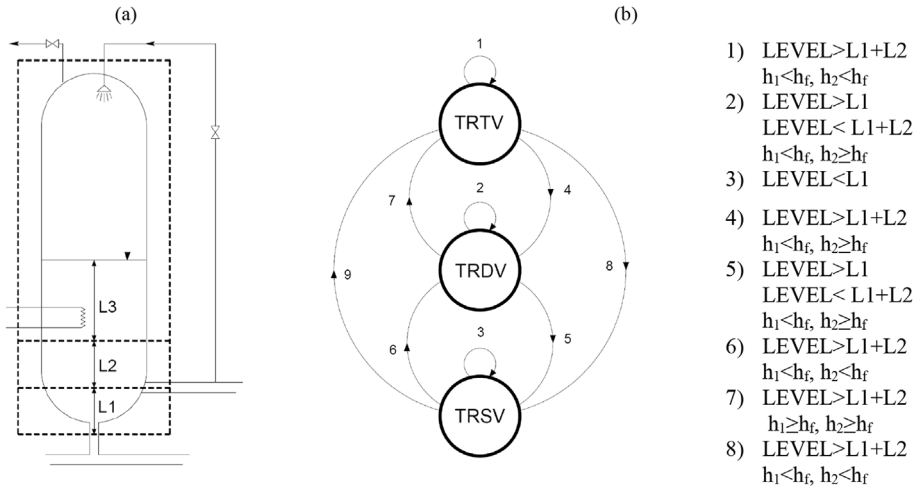

Fig. 2. Control volume sub division of the COM-MCV model (a) and switching logic between TRSV, TRDV and TRTV sub-models (b).

4.1. Two regions single volume sub-model (TRSV)

Starting from the TRSV sub-model (Tables 1 and 2 and Fig. 3), the necessary jump conditions can be defined by considering all the possible phenomena occurring across vapour and liquid phases.

In this regard, water and vapour regions can mutually transfer mass and energy thanks to vapour and liquid phase change induced by pressure and temperature variations. As for the mass and energy exchanges, they can take place owing to flashing, rainout, wall condensation and spray drops condensation. In addition, heat fluxes between the two regions can occur due to temperature differences between water and vapour at interface. Referring to Todreas and Kazimi (1990), for mass exchanges, the jump conditions are:

$$\dot{m}_v = \dot{m}_{FL} - \dot{m}_{RO} - \dot{m}_{SC} - \dot{m}_{WC}, \tag{1}$$

$$\dot{m}_l = -\dot{m}_{FL} + \dot{m}_{RO} + \dot{m}_{SC} + \dot{m}_{WC}, \tag{2}$$

where $\dot{m}$ is the mass flow rate. As for the subscripts, v represents the vapour phase and l the liquid one, while FL, RO, SC, and WC stay for flashing, rain out, superficial condensate on the spray drops and condensate on the pressurizer inner walls, respectively. As far as energy fluxes are concerned, if flashing (rainout) occurs at saturation conditions and the latent heat of evaporation (condensation) is supplied only by the liquid (vapour) region the energy jump conditions are:

$$\dot{m}_v h_v = \dot{m}_{FL} h_g, \tag{3}$$

$$\dot{m}_l h_l = -\dot{m}_{FL} h_f, \tag{4}$$

$$\dot{m}_v h_v = -\dot{m}_{RO} h_f, \tag{5}$$

$$\dot{m}_l h_l = \dot{m}_{RO} h_g, \tag{6}$$

where h is the specific enthalpy. g and f refer to the saturated vapour and saturated liquid, respectively.

Moreover, additional energy jump conditions can be obtained taking into account the condensation on spray drops. If the process occurs only at saturation conditions and the latent heat of condensation is released totally to the spray through the condensate shell, the following relations can be written as:

$$\dot{m}_v h_v = -\dot{m}_{SC} h_g, \tag{7}$$

$$\dot{m}_l h_l = \dot{m}_{SC} h_f. \tag{8}$$

In Eqs. (7) and (8), $\dot{m}_{SC}$ is connected to the water injected by the sprayers. Under the assumption that the rate of condensation is just sufficient to raise enthalpy of the spray to the saturation one, the following equation for $\dot{m}_{SC}$ can be obtained (Todreas and Kazimi, 1990; Kuridan and Beynon, 1998):

$$\dot{m}_{SC} = \dot{m}_{SP}\left(\frac{h_f - h_{SP}}{h_g - h_f}\right). \tag{9}$$

Eventually, by considering also the condensation on the pressurizer

Table 1
Possible thermodynamic state in the pressurizer for the TRSV sub-model.

State designation	TOP state	BOTTOM state
1	Superheated	Subcooled
2	Superheated	Saturated
3	Saturated	Subcooled
4	Saturated	Saturated

Table 2
State variables according to the different thermodynamic states TRSV sub-model.

State designation	State variables
1	$z = \{p, V_v, h_v, h_l\}^T$
2	$z = \{p, V_v, h_v, m_{FL}\}^T$
3	$z = \{p, V_v, m_{RO}, h_l\}^T$
4	$z = \{p, V_v, m_{RO}, m_{FL}\}^T$

wall, if it occurs only at saturation, the set of the energy jump conditions is completed by the following relation:

$$\dot{m}_v h_v = -\dot{m}_{WC} h_g. \tag{10}$$

In Eq. (10), $\dot{m}_{WC}$ is the wall condensate mass flow rate. By assuming that the latent heat of condensation released to condensate is completely transferred to the pressurizer wall, it is:

$$\dot{m}_{WC} = \frac{\dot{Q}_{WALL}}{(h_g - h_f)}. \tag{11}$$

In Eq. (11), $\dot{Q}_{WALL}$ is the total heat exchanged between the pressurizer volume and the walls.

At this point, using the information coming from the mass and energy jump conditions, the governing equations (mass and energy balance with the volume constraint[5]) for each state can be derived.

$$\dot{m}_v = \dot{m}_{FL} - \dot{m}_{RO} - \dot{m}_{CS} - \dot{m}_{VLV} - \dot{m}_{WC}, \tag{12}$$

$$\dot{m}_l = -\dot{m}_{FL} + \dot{m}_{RO} + \dot{m}_{SC} + \dot{m}_{SP} + \dot{m}_{WC} + \dot{m}_{INSURGE} - \dot{m}_{OUTSURGE}, \tag{13}$$

$$\dot{U}_v = \dot{m}_{FL}\cdot h_g - \dot{m}_{RO}\cdot h_f - \dot{m}_{CS}\cdot h_g - \dot{m}_{VLV}\cdot h_v - \dot{m}_{WC}\cdot h_g + - p\cdot\dot{V}_v - \dot{Q}_{vW} - \dot{Q}_{vl}, \tag{14}$$

$$\dot{U}_l = -\dot{m}_{FL}\cdot h_g + \dot{m}_{RO}\cdot h_f + \dot{m}_{SC}\cdot h_f + \dot{m}_{SP}\cdot h_f + \dot{m}_{WC}\cdot h_g + + \dot{m}_{INSURGE}\cdot h_{INSURGE} - \dot{m}_{OUTSURGE}\cdot h_l - p\cdot\dot{V}_l + \dot{Q}_H - \dot{Q}_{lW} + \dot{Q}_{vl}, \tag{15}$$

$$\dot{V} = 0, \tag{16}$$

$$\dot{V} = \dot{V}_v + \dot{V}_l = 0. \tag{17}$$

In Eqs. (14) and (15), $\dot{m}_{VLV}$ is the mass flow that can exit from the safety valve, U stays for the internal energy, V refers to the volume, $\dot{Q}_H$ is the heaters power, whereas the other $\dot{Q}$ terms are introduced to take into account energy exchange between different regions and heat losses from pressurizer tank to external environment. In this regard, $\dot{Q}_{vW}$ represents the heat exchange between the vapour phase and the pressurizer wall, $\dot{Q}_{lW}$ the heat exchange between the liquid phase and the pressurizer wall and $\dot{Q}_{vl}$ the heat exchange between the two phases. Each term has the same form of the Newton's law of cooling:

$$\dot{Q} = \alpha S \Delta T. \tag{18}$$

In Eq. (18), α is the convective heat transfer coefficient, S the exchange area, and ΔT the temperature difference. As for α, it is considered constant (equal to 100 W m $^{-2}$ °C $^{-1}$ with reference to Celata et al. (1986)), except for the computation of the wall condensate, for which the Nusselt theory is applied. In particular, when the vapour is saturated and the temperature T_{Win} of the internal side of pressurizer wall (of length L_{WALL}) is lower than the saturation one, the heat transfer coefficient, accordingly to Incropera and Dewitt (1996), can be computed as:

$$\alpha = 0.943\left[\frac{g\rho_l\left(\rho_l - \rho_g\right)h_{fg}' L_{WALL}^3}{k_l\mu_l(T_{sat} - T_{Win})}\right]^{\frac{1}{4}} \quad \text{with} \quad h_{fg}' = h_{fg}(1 + 0.68\cdot Ja), \tag{19}$$

where ρ, k and μ stay for the density, the thermal conductivity and the dynamics viscosity respectively. h_{fg} is the evaporation enthalpy, L_W the length of the wall and Ja the Jacob number, that is defined as:

$$Ja = \frac{C_{p,l}}{h_{fg}}(T_{sat} - T_{Win}). \tag{20}$$

It should be highlighted that, in Eq. (19), liquid properties must be evaluated at the film temperature.

$$T_{film} = \frac{T_{sat} + T_{Win}}{2} \tag{21}$$

and hence the pressurizer wall temperature has to be evaluated. To the purpose, the wall is divided into two shells, an internal one and an external one connected by a thermal resistance.

$$C_{Win}\frac{dT_{Win}}{dt} = \dot{Q}_{lW} + \dot{Q}_{vW} - \dot{Q}_{cond}, \quad C_{Wout}\frac{dT_{out}}{dt} = \dot{Q}_{cond} - \dot{Q}_{ext}. \tag{22}$$

In Eq. (22), C_{Win} and C_{Wout} refer to the heat capacity of the inner and outer shell of the pressurizer wall, respectively. $\dot{Q}_{cond}$ is the heat transfer due to the thermal conduction in the wall, while $\dot{Q}_{ext}$ represents the thermal losses to the environment.

The ensemble of Eqs. 12–17 gives rise to a nonlinear Differential Algebraic Equation (DAE) system. In particular, it belongs to a particular subclass of DAEs (more details can be found in Petzold (1982) and Ascher and Petzold (1998)), called Ordinary Differential Equation (ODE) system with constraints. In this case, there is a single constraint: the conservation of the pressurizer volume. If the vapour and liquid volumes are expressed as

$$V_v = \frac{m_v}{\rho_v}, \tag{23}$$

$$V_l = \frac{m_l}{\rho_l}, \tag{24}$$

and then V_v and V_l are differentiated with respect to time, the algebraic constraint becomes a system of two ODEs:

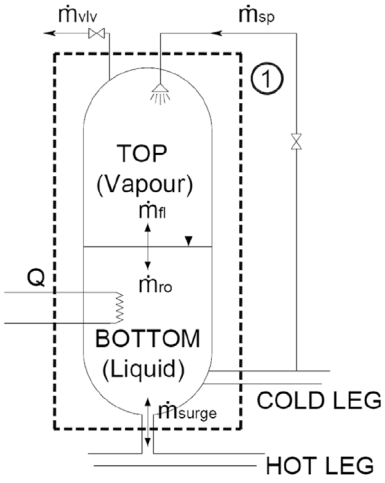

Fig. 3. Top region (Vapour) and Bottom region (Liquid) of TRSV sub-model.

[5] The pressurizer volume does not change.

Table 3
Possible thermodynamic states in the pressurizer for the TRDV sub-model.

State designation	TOP state	MIDDLE state	BOTTOM state
1	Superheated	Subcooled	Subcooled
2	Superheated	Saturated	Subcooled
3	Saturated	Subcooled	Subcooled
4	Saturated	Saturated	Subcooled

$$\dot{V}_v \cdot \rho_v + V_v \cdot \dot{\rho}_v = \dot{m}_{vV}, \tag{25}$$

$$\dot{V}_l \cdot \rho_l + V_l \cdot \dot{\rho}_l = \dot{m}_l. \tag{26}$$

Moreover, by using the mass balance, Eqs. (25) and (26) can be written in the following form:

$$\dot{V}_v \cdot \rho_v + V_v \cdot \dot{\rho}_v - \dot{m}_{RO} + \dot{m}_{WC} + \dot{m}_{FL} = -\dot{m}_{SC} - \dot{m}_{VLV}, \tag{27}$$

$$\dot{V}_l \cdot \rho_l + V_l \cdot \dot{\rho}_l + \dot{m}_{FL} - \dot{m}_{RO} = \dot{m}_{SC} + \dot{m}_{WC} + \dot{m}_{SP} + \dot{m}_{INSURGE} - \dot{m}_{OUTSURGE}. \tag{28}$$

As far as the energy balance is concerned, Eqs. (14) and (15) can be expressed in terms of pressure and enthalpy, taking into account the following well known relation:

$$u = h - pv, \tag{29}$$

where u is the specific internal energy.

Then, by substituting Eq. (29) in Eqs. the energy balance for vapour and water becomes:

$$m_v \cdot \dot{h}_v - \dot{p} \cdot V_v - \dot{m}_{FL} \cdot (h_g - h_v) + \dot{m}_{RO} \cdot (h_f - h_v) = -\dot{m}_{SC} \cdot (h_g - h_v) - \dot{m}_{WC} \cdot (h_g - h_v) - \dot{Q}_{vW} - \dot{Q}_{vl}, \tag{30}$$

$$m_l \cdot \dot{h}_l - \dot{p} \cdot V_l + \dot{m}_{FL} \cdot (h_g - h_l) - \dot{m}_{RO} \cdot (h_f - h_l) = \dot{m}_{SC} \cdot (h_f - h_l) + \dot{m}_{WC} \cdot (h_g - h_l) + \dot{m}_{SP} \cdot (h_f - h_l) + \dot{m}_{INSURGE} \cdot (h_{INSURGE} - h_l) + \dot{Q}_H - \dot{Q}_{lW} + \dot{Q}_{vl}. \tag{31}$$

Eventually, density and enthalpy time derivatives appearing in Eqs. (30) and (31) is made explicit as follows:

$$if\ h_l < h_f\ or\ h_v > h_g \quad \rho = \rho(p, h) \rightarrow \frac{d\rho}{dt} = \frac{\partial \rho}{\partial p}\frac{dp}{dt} + \frac{\partial \rho}{\partial h}\frac{dh}{dt} = \frac{\partial \rho}{\partial p}\dot{p} + \frac{\partial \rho}{\partial h}\dot{h}, \tag{32}$$

$$if\ h_l = h_f\ or\ h_v = h_g \quad \rho = \rho(p) \rightarrow \frac{d\rho}{dt} = \frac{d\rho}{dp}\frac{dp}{dt} = \frac{d\rho}{dp}\dot{p}, \tag{33}$$

$$if\ h_l = h_f\ or\ h_v = h_g \quad h = h(p) \rightarrow \frac{dh}{dt} = \frac{dh}{dp}\frac{dp}{dt} = \frac{dh}{dp}\dot{p}. \tag{34}$$

In this way, the original DAE system has been converted into an ODE one, and all the state variables of the pressurizer are pointed out. In particular, state variables can be singled out from all the other terms using the following matrix formulation:

$$\Psi(z) \cdot \dot{z} = \eta. \tag{35}$$

In Eq. (35), $\dot{z}$ is the vector of the time derivatives of the state variables and η the vector of the input variables. For brevity, the matrix formulation is shown in the Appendix.

Due to the different thermodynamic states, which can exist within the pressurizer (according to Table 1), also the state variables can change. For subcooled and superheated states, the state variables of the system are the pressure, the enthalpy of liquid and vapour and the vapour volume. The choice of vapour volume instead of the liquid one is arbitrary. At saturation condition, enthalpy cannot be a state variable, since it depends on pressure. The state variables characterizing the system for each thermodynamic state are reported in Table 2.

4.2. Two regions double volume sub-model (TRDV)

Following the same procedure, the TRDV sub-model (Figs. 4 and 5 and Tables 3 and 4) governing equations can be obtained (the jump condition do not change). In this case, mass and energy balances must be separately written for in-surge transients and for out-surge ones, since the boundary between control volume ① and the liquid region of control volume ② allows for bidirectional exchanges of water. During in-surge transients, the water coming from the cold leg of the primary loop enters volume ① and pushes the water filling it into volume ② (see Fig. 4a). During out-surge transients, the water coming from volume ① to the cold leg, draws the water contained in volume ② to volume ① (see Fig. 4b). For in-surges, the governing equations are:

$$\dot{V}_{2v} \cdot \rho_{2v} + V_{2v} \cdot \dot{\rho}_{2v} - \dot{m}_{FL} + \dot{m}_{RO} = -\dot{m}_{SC} - \dot{m}_{VLV} - \dot{m}_{WC}, \tag{36}$$

$$\dot{V}_{2l} \cdot \rho_{2l} + V_{2l} \cdot \dot{\rho}_{2l} + \dot{m}_{FL} - \dot{m}_{RO} - \dot{m}_{OUT_1} = \dot{m}_{SC} + \dot{m}_{WC} + \dot{m}_{SP}, \tag{37}$$

$$V_1 \cdot \dot{\rho}_1 - \dot{m}_{OUT_1} = \dot{m}_{INSURGE}, \tag{38}$$

$$m_{2v} \cdot \dot{h}_{2v} - \dot{p} \cdot V_{2v} - \dot{m}_{FL} \cdot (h_g - h_{2v}) + \dot{m}_{RO} \cdot (h_f - h_{2v}) = -\dot{m}_{SC} \cdot (h_g - h_{2v}) - \dot{m}_{WC} \cdot (h_g - h_{2v}) - \dot{Q}_{2v2l} - \dot{Q}_{2vW}, \tag{39}$$

$$m_{2l} \cdot \dot{h}_{2l} - \dot{p} \cdot V_{2l} + \dot{m}_{FL} \cdot (h_g - h_{2l}) - \dot{m}_{RO} \cdot (h_f - h_{2l}) - \dot{m}_{OUT.1} \cdot (h_1 - h_{2l}) = \dot{m}_{SC} \cdot (h_f - h_{2l}) + \dot{m}_{SP} \cdot (h_f - h_{2l}) + \dot{m}_{WC} \cdot (h_g - h_{2l}) + \dot{Q}_{2v2l} - \dot{Q}_{2l1} - \dot{Q}_{2lW} + \dot{Q}_H, \tag{40}$$

$$m_1 \dot{h}_1 - \dot{p} \cdot V_1 = \dot{m}_{INSURGE}(h_{INSURGE} - h_1) + \dot{Q}_{2l1} - \dot{Q}_{1W}, \tag{41}$$

while, for the out-surge ones:

$$\dot{V}_{2v} \cdot \rho_{2v} + V_{2v} \cdot \dot{\rho}_{2v} - \dot{m}_{FL} + \dot{m}_{RO} = -\dot{m}_{SC} - \dot{m}_{VLV} - \dot{m}_{WC}, \tag{42}$$

$$\dot{V}_{2l} \cdot \rho_{2l} + V_{2l} \cdot \dot{\rho}_{2l} + \dot{m}_{FL} - \dot{m}_{RO} + \dot{m}_{OUT_2} = \dot{m}_{SC} + \dot{m}_{WC} + \dot{m}_{SP}, \tag{43}$$

$$V_1 \cdot \dot{\rho}_1 - \dot{m}_{OUT_2} = -\dot{m}_{OUTSURGE}, \tag{44}$$

$$m_{2v} \cdot \dot{h}_{2v} - \dot{p} \cdot V_{2v} - \dot{m}_{FL} \cdot (h_g - h_{2v}) + \dot{m}_{RO} \cdot (h_f - h_{2v}) = -\dot{m}_{SC} \cdot (h_g - h_{2v}) - \dot{m}_{WC} \cdot (h_g - h_{2v}) - \dot{Q}_{2v2l} - \dot{Q}_{2vW}, \tag{45}$$

$$m_{2l} \cdot \dot{h}_{2l} - \dot{p} \cdot V_{2l} + \dot{m}_{FL} \cdot (h_g - h_{2l}) - \dot{m}_{RO} \cdot (h_f - h_{2l}) = \dot{m}_{SC} \cdot (h_f - h_{2l}) + \dot{m}_{SP} \cdot (h_f - h_{2l}) + \dot{m}_{WC} \cdot (h_g - h_{2l}) + \dot{Q}_{2v2l} - \dot{Q}_{2l1} - \dot{Q}_{3lW} + \dot{Q}_H, \tag{46}$$

$$m_1 \dot{h}_1 - \dot{p} \cdot V_1 - \dot{m}_{OUT_2}(h_{2l} - h_1) = \dot{Q}_{2l1} - \dot{Q}_{1W}, \tag{47}$$

In Eqs. 36–47, $\dot{m}_{OUT_1}$ is the liquid water mass flow rate entering from

Table 4
State variables according to the different thermodynamic states for TRDV sub-model.

In-surge transients		5	Out-surge transients
State designation	State variables	State designation	State variables
1	$z = \{p, V_{2v}, h_{2v}, h_{2l}, h_1, h_2, m_{OUT.1}\}^T$	1	$z = \{p, V_{2v}, h_{2v}, h_{2l}, h_1, h_2, m_{OUT.2}\}^T$
2	$z = \{p, V_{2v}, h_{2v}, m_{FL}, h_1, h_2, m_{OUT.1}\}^T$	2	$z = \{p, V_{2v}, h_{2v}, m_{FL}, h_1, h_2, m_{OUT.2}\}^T$
3	$z = \{p, V_{2v}, m_{RO}, h_{2l}, h_1, h_2, m_{OUT.1}\}^T$	3	$z = \{p, V_{2v}, m_{RO}, h_{2l}, h_1, h_2, m_{OUT.2}\}^T$
4	$z = \{p, V_{2v}, m_{RO}, m_{FL}, h_1, h_2, m_{OUT.1}\}^T$	4	$z = \{p, V_{2v}, m_{RO}, m_{FL}, h_1, h_2, m_{OUT.2}\}^T$

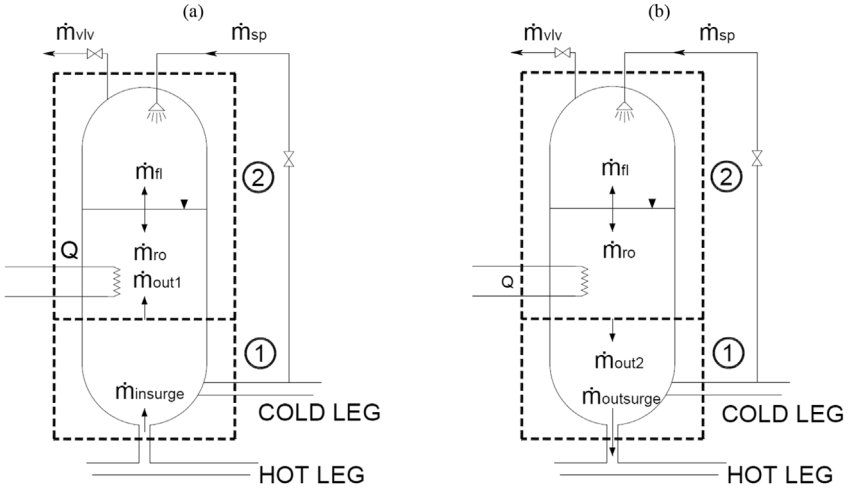

Fig. 4. TRDV sub-model for in-surge transients (a) and for out-surge ones (b).

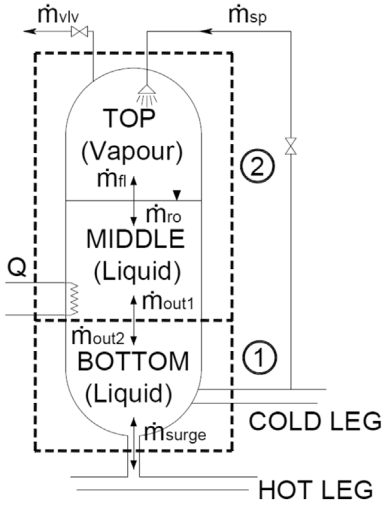

Fig. 5. Top region (Vapour), middle region (Liquid) and bottom region (Liquid) of TRDV sub-model.

volume ① to volume ② during in-surge transients, while $\dot{m}_{OUT_2}$ is the liquid water mass flow rate exiting from volume ② to volume ① in case of out-surge. The terms labelled with the letter $\dot{Q}$ are:

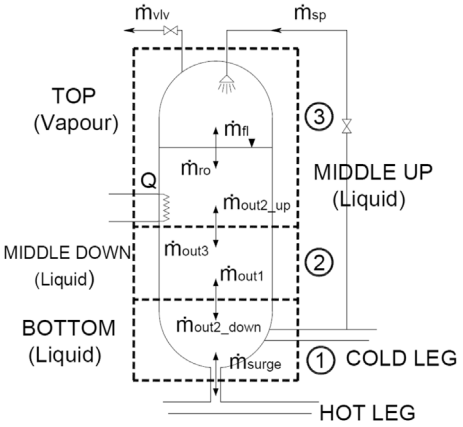

Fig. 7. Top region (Vapour), middle region (Liquid) and bottom region (Liquid) of TRDV sub-model.

- Heat exchange between volume ① and liquid region of volume ②

$$\dot{Q}_{2l1} = \alpha_{2l1} S (T_{2l} - T_1). \tag{48}$$

- Heat exchange between liquid and vapour region of volume ②

$$\dot{Q}_{2v2l} = \alpha_{2v2l} S (T_{2v} - T_{l2}). \tag{49}$$

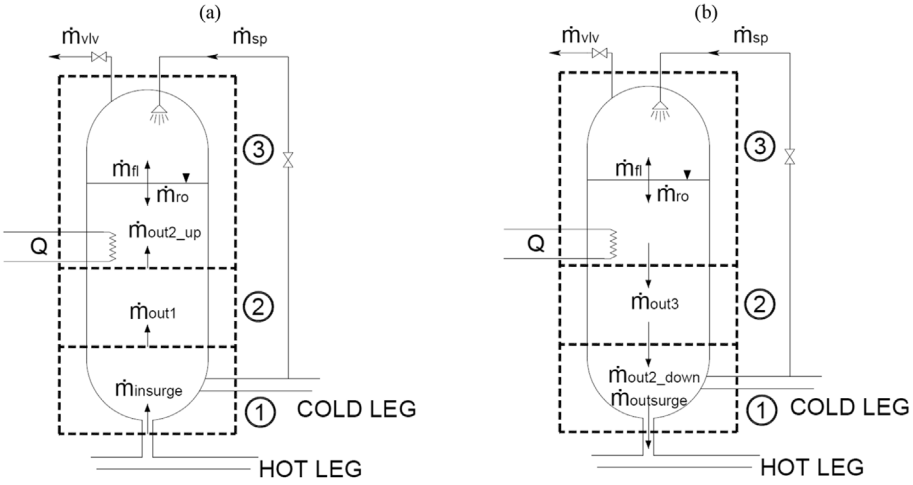

Fig. 6. TRTV sub-model for in-surge transients (a) and for out-surge ones (b).

Table 5
Possible thermodynamic states in the pressurizer for the TRTV sub-model.

State designation	TOP state	MIDDLE UP state	MIDDLE DOWN state	DOWN state
1	Superheated	Subcooled	Subcooled	Subcooled
2	Superheated	Saturated	Subcooled	Subcooled
3	Saturated	Subcooled	Subcooled	Subcooled
4	Saturated	Saturated	Subcooled	Subcooled

- Heat exchange between volume ① and the pressurizer wall

$$\dot{Q}_{1W} = \alpha_{1W} S_1 (T_1 - T_W). \tag{50}$$

- Heat exchange between liquid region of volume ② and the pressurizer wall

$$\dot{Q}_{2lW} = \alpha_{2lW} S_{2l} (T_{2l} - T_W). \tag{51}$$

- Heat exchange between vapour region of volume ② and the pressurizer wall

$$\dot{Q}_{2vW} = \alpha_{2vW} S_{2v} (T_{2v} - T_W). \tag{52}$$

As for the value of the heat transfer coefficients, they have been considered equal to 100 W m $^{-2}$°C $^{-1}$ with reference to Celata et al. (1986). In Table 3 (referring to Fig. 5), the possible thermodynamic states that can occur in the different regions are reported. The state variables describing the system according to a given thermodynamic condition are collected in Table 4.

4.3. Two regions triple volume sub-model (TRTV)

In this Section, the governing equations of the TRTV sub-model (Figs. 6 and 7 and Tables 5 and 6) are presented. Also in this case, mass and energy balances must be separately written for in-surge transients and for out-surge ones, due to the presence of the boundaries between control volumes①,②,③ and ƒ (Fig. 6).

For the in-surge transients, the governing equations are:

$$\dot{V}_{3v} \cdot \rho_{3v} + V_{3v} \cdot \dot{\rho}_{3v} - \dot{m}_{FL} + \dot{m}_{RO} = -\dot{m}_{SC} - \dot{m}_{VLV} - \dot{m}_{WC}, \tag{53}$$

$$\dot{V}_{3l} \cdot \rho_{3l} + V_{3l} \cdot \dot{\rho}_{3l} + \dot{m}_{FL} - \dot{m}_{RO} - \dot{m}_{OUT_{2_{up}}} = \dot{m}_{SC} + \dot{m}_{SP} + \dot{m}_{WC}, \tag{54}$$

$$V_{2v} \cdot \dot{\rho}_{2v} - \dot{m}_{OUT_1} + \dot{m}_{OUT_{2_{up}}} = 0, \tag{55}$$

$$V_{1v} \cdot \dot{\rho}_{1v} + \dot{m}_{OUT_1} = \dot{m}_{INSURGE}, \tag{56}$$

$$m_{3v} \cdot \dot{h}_{3v} - \dot{p} \cdot V_{3v} - \dot{m}_{FL} \cdot (h_g - h_{3v}) + \dot{m}_{RO} \cdot (h_f - h_{3v}) = -\dot{m}_{SC} \cdot (h_g - h_{3v}) - \dot{m}_{WC} \cdot (h_g - h_{3v}) - \dot{Q}_{3v3l} - \dot{Q}_{3vW}, \tag{57}$$

$$m_{3l} \cdot \dot{h}_{3l} - \dot{p} \cdot V_{3l} + \dot{m}_{FL} \cdot (h_g - h_{3l}) - \dot{m}_{RO} \cdot (h_f - h_{3l}) - \dot{m}_{OUT.2.up} \cdot (h_2 - h_{3l}) = \dot{m}_{SC} \cdot (h_f - h_{3l}) + \dot{m}_{SP} \cdot (h_f - h_{3l}) + \dot{m}_{WC} \cdot (h_g - h_{3l}) - \dot{Q}_{3l2} + \dot{Q}_{3v3l} - \dot{Q}_{3lW} + \dot{Q}_H, \tag{58}$$

$$m_2 \dot{h}_2 - \dot{p} \cdot V_2 - \dot{m}_{OUT_1} (h_1 - h_2) = -\dot{Q}_{21} + \dot{Q}_{3l2} - \dot{Q}_{2W}, \tag{59}$$

$$m_1 \dot{h}_1 - \dot{p} \cdot V_1 = \dot{m}_{INSURGE} (h_{INSURGE} - h_1) + \dot{Q}_{21} - \dot{Q}_{1W}, \tag{60}$$

while for then out-surge transients, the following set of balances can be obtained:

$$\dot{V}_{3v} \cdot \rho_{3v} + V_{3v} \cdot \dot{\rho}_{3v} - \dot{m}_{FL} + \dot{m}_{RO} = -\dot{m}_{SC} - \dot{m}_{VLV} - \dot{m}_{WC}, \tag{61}$$

$$\dot{V}_{3l} \cdot \rho_{3l} + V_{3l} \cdot \dot{\rho}_{3l} + \dot{m}_{FL} - \dot{m}_{RO} - \dot{m}_{OUT_3} = \dot{m}_{SC} + \dot{m}_{SP} + \dot{m}_{WC}, \tag{62}$$

$$V_{2v} \cdot \dot{\rho}_{2v} - \dot{m}_{OUT_3} + \dot{m}_{OUT_{2_{down}}} = 0, \tag{63}$$

$$V_{1v} \cdot \dot{\rho}_{1v} - \dot{m}_{OUT_{2_{down}}} = -\dot{m}_{OUTSURGE}, \tag{64}$$

$$m_{3v} \cdot \dot{h}_{3v} - \dot{p} \cdot V_{3v} - \dot{m}_{FL} \cdot (h_g - h_{3v}) + \dot{m}_{RO} \cdot (h_f - h_{3v}) = -\dot{m}_{SC} \cdot (h_g - h_{3v}) - \dot{m}_{WC} \cdot (h_g - h_{3v}) - \dot{Q}_{3v3l} - \dot{Q}_{3vW}, \tag{65}$$

$$m_{3l} \cdot \dot{h}_{3l} - \dot{p} \cdot V_{3l} + \dot{m}_{FL} \cdot (h_g - h_{3l}) - \dot{m}_{RO} \cdot (h_f - h_{3l}) = \dot{m}_{SC} \cdot (h_f - h_{3l}) + \dot{m}_{SP} \cdot (h_f - h_{3l}) + \dot{m}_{WC} \cdot (h_g - h_{3l}) - \dot{Q}_{3l2} + \dot{Q}_{3v3l} - \dot{Q}_{3lW} + \dot{Q}_H, \tag{66}$$

$$m_2 \dot{h}_2 - \dot{p} \cdot V_2 - \dot{m}_{OUT_{3l}} (h_{3l} - h_2) = -\dot{Q}_{21} + \dot{Q}_{3l2} - \dot{Q}_{2W}, \tag{67}$$

$$m_1 \dot{h}_1 - \dot{p} \cdot V_1 - \dot{m}_{OUT_{2_{down}}} (h_2 - h_1) = \dot{Q}_{21} - \dot{Q}_{1W}. \tag{68}$$

During in-surges, $\dot{m}_{OUT_1}$ is the liquid water mass flow rate coming from volume ① to volume ② and $\dot{m}_{OUT_{2up}}$ the liquid water mass flow rate coming from volume ② to volume ③. On the contrary, during out-surges, $\dot{m}_{OUT_3}$ is the liquid water mass flow rate coming from volume ③ to volume ② and $\dot{m}_{OUT_{2_{down}}}$ is the liquid water mass flow rate coming from volume ② to volume ①. In order to help the comprehension of the.

TRTV sub-model, the mass exchanges that can occur are summarized in Fig. 7. As for the heat exchange (the heat transfer coefficients have been considered equal to 100 W m $^{-2}$°C^{-1} with reference to Celata et al. (1986)), $\dot{Q}$ terms are.

- Heat exchange between volume ① and volume ②

$$\dot{Q}_{12} = \alpha_{12} S (T_{2l} - T_{1l}). \tag{69}$$

- Heat exchange between volume ② and liquid region of volume ③

$$\dot{Q}_{3l2} = \alpha_{3l2} S (T_{3l} - T_2). \tag{70}$$

- Heat exchange between liquid and vapour region of volume ③

$$\dot{Q}_{3v3l} = \alpha_{3v3l} S (T_{3v} - T_{3l}). \tag{71}$$

- Heat exchange between volume ① and the pressurizer wall

$$\dot{Q}_{1W} = \alpha_{1W} S_1 (T_1 - T_W). \tag{72}$$

- Heat exchange between volume ② and the pressurizer wall

$$\dot{Q}_{2W} = \alpha_{2W} S_2 (T_2 - T_W). \tag{73}$$

- Heat exchange between liquid region of volume ③ and the pressurizer wall

Table 6
State variables according to the different thermodynamic states for TRTV model.

In-surge transients		Out-surge transients	
State	State variables	State	State variables
1	$z = \{p, V_{3v}, h_{3v}, h_{3l}, h_1, h_2, m_{OUT.2.up}, m_{OUT.1}\}^T$	1	$z = \{p, V_{3v}, h_{3v}, h_{3l}, h_1, h_2, m_{OUT.2.down}, m_{OUT.3}\}^T$
2	$z = \{p, V_{3v}, h_{3v}, m_{FL}, h_1, h_2, m_{OUT.2.up}, m_{OUT.1}\}^T$	2	$z = \{p, V_{3v}, h_{3v}, m_{FL}, h_1, h_2, m_{OUT.2.down}, m_{OUT.3}\}^T$
3	$z = \{p, V_{3v}, m_{RO}, h_{3l}, h_1, h_2, m_{OUT.2.up}, m_{OUT.1}\}^T$	3	$z = \{p, V_{3v}, m_{RO}, h_{3l}, h_1, h_2, m_{OUT.2.down}, m_{OUT.3}\}^T$
4	$z = \{p, V_{3v}, m_{RO}, m_{FL}, h_1, h_2, m_{OUT.2.up}, m_{OUT.1}\}^T$	4	$z = \{p, V_{3v}, m_{RO}, m_{FL}, h_1, h_2, m_{OUT.2.down}, m_{OUT.3}\}^T$

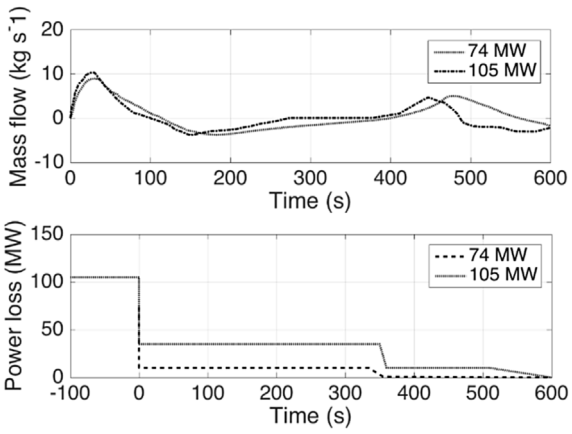

Fig. 8. 74 MWe (top) and 105 MWe (bottom) loss of load transient.

Table 7
Shippingport pressurizer geometrical data (Redfield et al., 1967).

D (m)	H (m)	V (m^3)	V of vapour (m^3)	p (bar)	Spray temperature (°C)
1.37	5.1	7.419	3.7	142	260

Table 8
Shippingport pressure control system.

Spray flow rate (kg/s)	1.91	Turn ON p (bar)	143	Shut OFF p (bar)	140
Heating Rating Bank 1 (kw)	40	Turn ON T (°C)	332	Turn OFF T (°C)	336
Heating Rating Bank 1 (kw)	80	Turn ON p (bar)	134	Shut OFF p (bar)	138
Heating Rating Bank 1 (kw)	250	Turn ON p (bar)	131	Shut OFF p (bar)	139

$$\dot{Q}_{3lW} = \alpha_{3lW} S_{3l} (T_{3l} - T_W). \tag{74}$$

- Heat exchange between vapour region of volume ③ and the pressurizer wall

$$\dot{Q}_{3vW} = \alpha_{3vW} S_{3v} (T_{3v} - T_W). \tag{75}$$

Table 5, according to Fig. 7, reports the thermodynamic states that can be experimented by the different regions. In Table 6, the state variable for the possible states are shown.

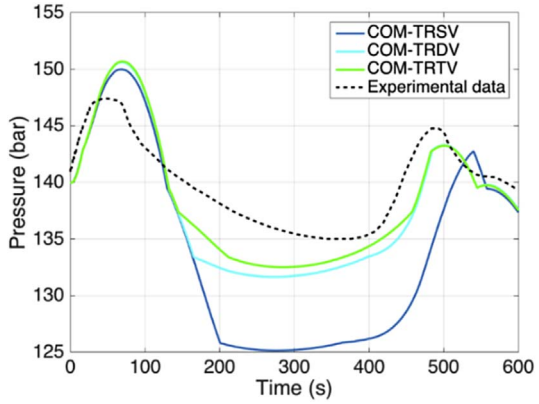

Fig. 10. 74 MWe loss of load TRSV, TSDV, TRTV pressure results.

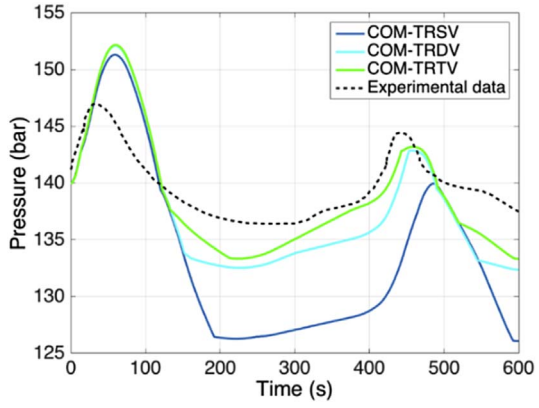

Fig. 11. 105 MWe loss of load TRSV, TSDV, TRTV pressure results.

5. Model validation

The mathematical formulation presented in the previous sections can be implemented in a MATLAB/Simulink® routine. In order to validate the code, Shippingport pressurizer experimental data during loss of load have been selected (Redfield et al., 1967).

In particular, two loss of load transients are simulated (see Fig. 8):

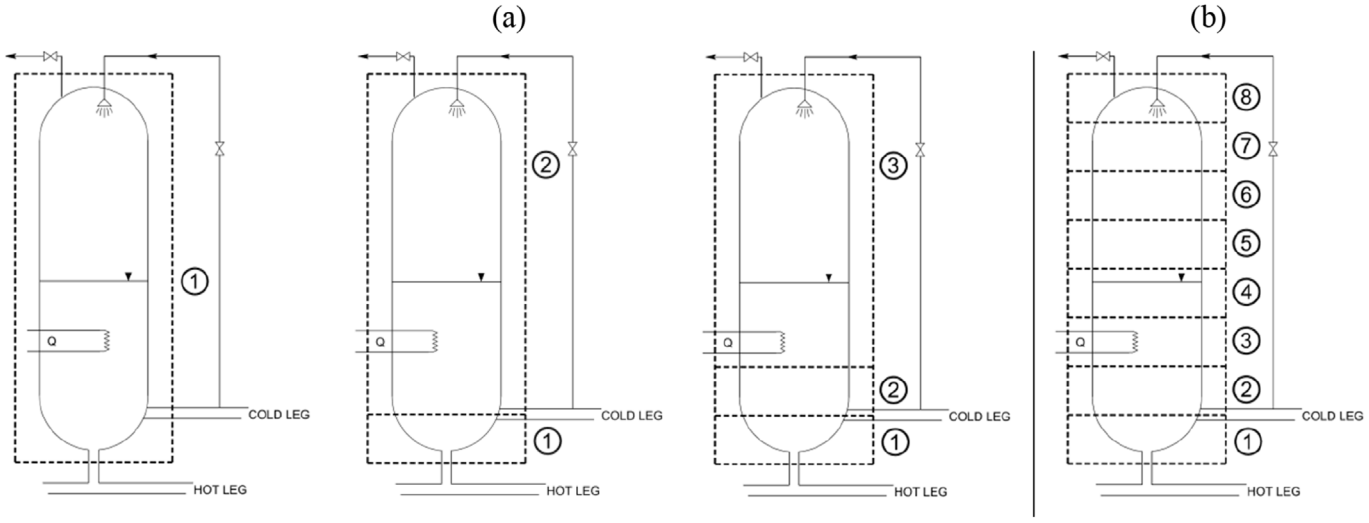

Fig. 9. COM-MCV (a) and RELAP5 (b) control volumes comparison.

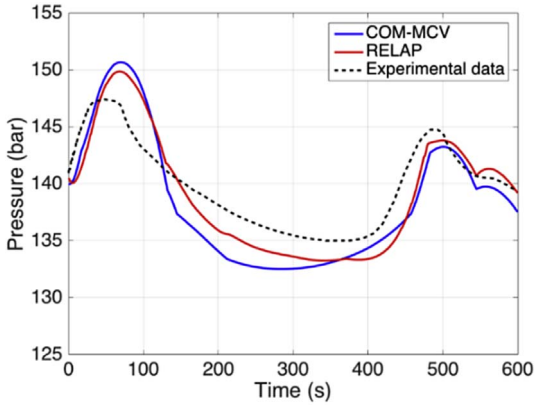

Fig. 12. 74 MWe loss of load new COM and RELAP5 pressure results.

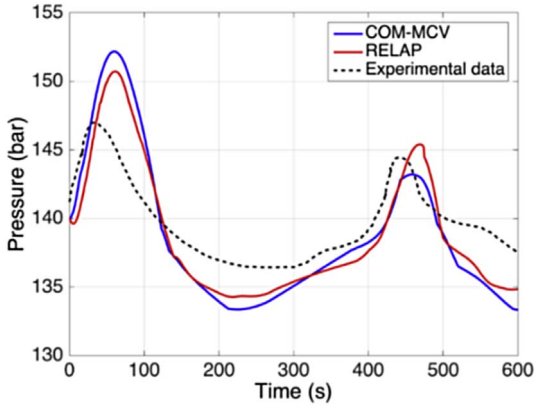

Fig. 13. 105 MWe loss of load new COM and RELAP5 pressure results.

- Loss of load from 74 MWe.
- Loss of load from 105 MWe.

The Shippingport pressurizer is cylindrical, with a diameter of 1.371 m and a total volume of 7.419 m^3. Pressure is maintained within control by three banks of electrical heaters, a spray system, and both vapour and water relief valves. The pressurizer geometrical data and initial conditions are given in Table 7. The pressure control operations (heaters and sprayers) are summarized in Table 8.

First, TRSV, TRDV and TRTV sub-models are decoupled from the COM-MCV and the results coming from each sub-model are compared with each another. Then the complete COM-MCV (TRSV + TRDV + TRTV) accuracy is tested. Besides, COM-MCV results are compared with a RELAP5 pressurizer model, which is used as standard reference for a code to code comparison.

Table 9
Comparison between the computational time of the COM-MCV and RELAP5 models (single core utilization of a machine adopting an Intel Core i7 with a clock speed of 2.3 GHz).

Transient	Simulated time (s)	COM-MCV simulation time (s)	RELAP5 simulation time (s)
74 MWe	600	58	345
105 MWe	600	75	405

RELAP5 model is based on the selection of eight control volumes. Starting from the bottom, the first RELAP5 control volume corresponds to volume ① of TRTV and TRDV sub-models, whereas the second RELAP5 control volume corresponds to volume ② of the TRTV sub-model (see Fig. 9).

Figs. 10 and 11 compare pressure experimental data with the results of TRSV, TRDV and TRTV sub-models. TRDV and TRTV sub-models show a quite good agreement with experimental data, on the contrary the TRSV does not reproduce accurately the test transient. This behaviour is related to an axial temperature distributions arising in the liquid phase during in-surge transients. In particular, the temperature experimentally measured at 1.5 m from the bottom of the pressurizer is much different from that of the in-surge water. On the contrary, in vapour region, no temperature distributions occur.

Figs. 12 and 13 show a comparison between pressure experimental data, the complete COM-MCV and RELAP5 pressurizer model. The accuracy of the COM-MCV is comparable with that of the RELAP5 one.

Fig. 14 compares experimental, complete COM-MCV and RELAP5 temperature distributions inside the liquid phase. Since, the experimental temperature values refer to the water present near the liquid vapour interface, they are compared with temperature computed in the upper control volumes of COM-MCV and RELAP5 model.

As for the computational burden, in Table 9 the computational times required for the COM and the RELAP5 models are reported. It is possible to notice (by considering a single core utilization of a personal computer with an Intel Core i7 with a clock speed of 2.3 GHz), that the simulations of the Shippingport transients by means of the RELAP5 model take some minutes while the COM model presented in this work runs in about 1 min. This fact is very important for testing and optimization of different control schemes.

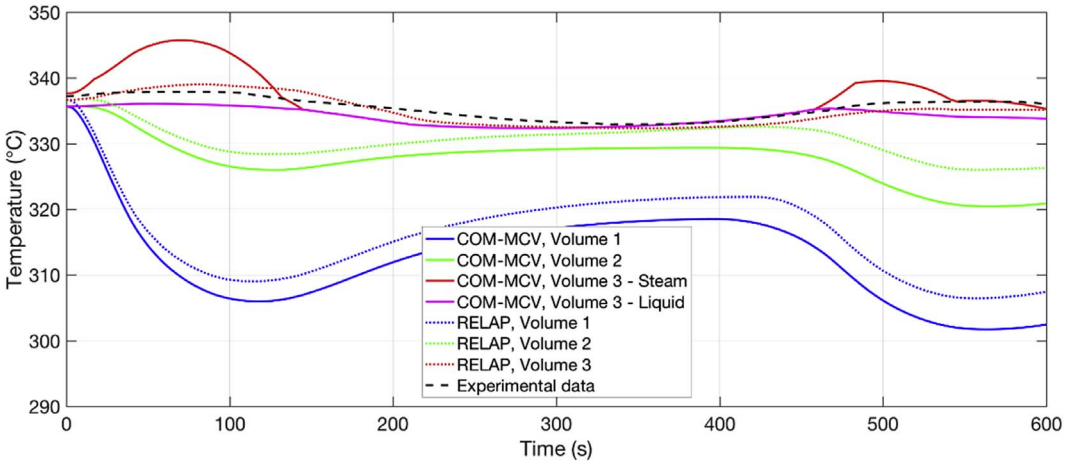

Fig. 14. 74 MWe loss of load new COM and RELAP5 liquid phase temperature distribution results. The experimental data refers to the temperature measured at 1.5 m from the bottom of the pressurizer.

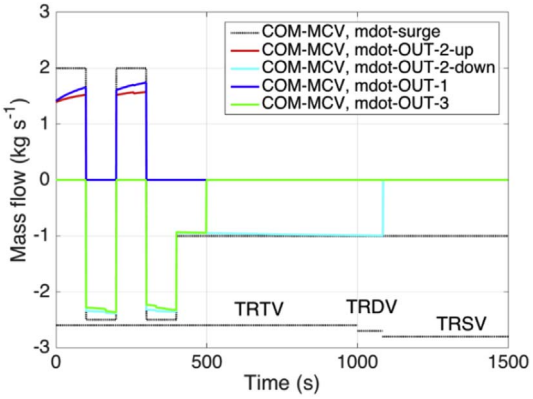

Fig. 15. Test transient (dotted line) and mass flow between different control volume of COM-MCV. The dotted lines refer to the selected sub-model during the simulation.

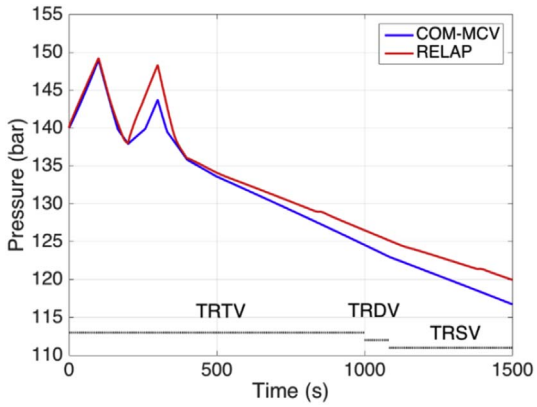

Fig. 16. COM-MCV vs. RELAP5 pressure transient results. The dotted lines refer to the selected sub-model during the simulation.

6. A complete emptying out-surge transient

According to the previous results, the MCV formulation is necessary in order to achieve good accuracy levels. In literature, COMs employing the MCV approach are present (e.g., see Botelho et al. (2010) for more details). Such models are usually based on the selection of two or three control volumes, one of which is divided into two regions (one for vapour and the other for water) with automatic changing of thermodynamic states. The remaining control volumes are fixed thermodynamic regions for subcooled water. If the water contained in the lower control volume remains in the subcooled state, this kind of COMs are suitable to reproduce faithfully pressurizer transients. However, if the water of the lower control volume reaches the saturation condition, such models are no longer able to reproduce any transient. The possibility that water reaches the saturated state also at the bottom of the pressurizer may occur during complete emptying out-surge transients. The capability to reproduce this kind of transients for a COM is important to develop and optimize control approaches which can help to reduce damages to the nuclear plant. Once the most promising control strategy has been selected, its effectiveness can be verified by adopting a SOM. Therefore, COMs and SOMs should be intended as complementary (and not mutually exclusive) approaches to achieve high safety and performance levels for a given system.

Simulations of the complete pressurizer emptying can be carried on by the COM-MCV developed in this study thanks to the coupling of the TRSV, TSDV and TRTV sub-models (see Section 2 for more details). In order to verify the accuracy of the model for complete emptying out-surges, new COM results are compared with RELAP5 ones. The selected test transient is reported in Fig. 15 (dotted line). Fig. 16 shows the comparison between COM-MCV and RELAP5 pressure results confirming the good accuracy of the model developed in this study. The difference between new COM-MVC and RELAP5 pressure simulations does not exceed 2 3 bars. Fig. 17 depicts temperature values of the COM-MCV and RELAP5 corresponding volumes: the maximum difference does not overcome 4 5 °C. Figs. 15–17 also report the number of control volumes adopted by the new COM-MVC during the simulation.

7. Conclusions

A new control oriented model, namely the COM-MCV, for PWRs pressurizer is developed. Thanks to the non-equilibrium approach and to the innovative multiple control volume formulation, the new model is suitable for the prediction of pressure and temperature behaviour inside the pressurizer for every transient that can be experimented by the system.

Experimental and simulated results point out that the axial temperature distribution arising in the liquid region cannot be neglected in order to obtain a model characterized by a satisfying level of accuracy. For this reason, single volume models are not suitable to study the pressurizer dynamics and multiple control volumes ones have to be adopted. Simulations also show that water laying in the bottom regions of the pressurizer can reach the saturated condition in case of severe out-surge transients.

This occurrence refers to single volume models, since the multiple control volumes ones cannot be employed if lower control volumes reach the saturation. In order to overcome single and multiple control volumes models limitations, the new model couples the two different approaches.

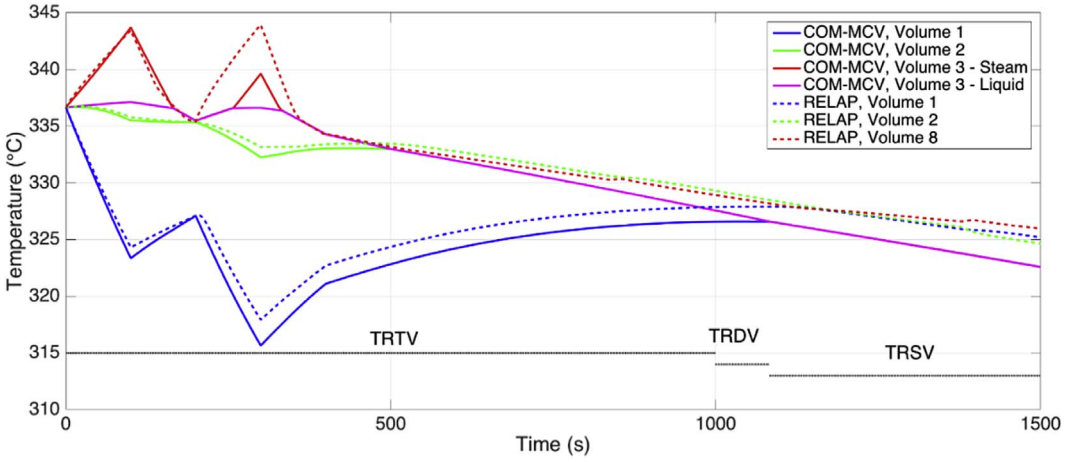

Fig. 17. COM-MCV vs. RELAP5 temperature transient results. The dotted lines refer to the selected sub-model during the simulation.

As for the future developments, in order to improve the accuracy of the model, the developed COM-MCV will be tested by coupling it to a PWR-simulator in order to relax the hypothesis of constant enthalpy for the mass flow rate entering in the pressurize. In addition, the obtained results will be compared with those that will be achieve thanks to a CFD pressurizer model which is under development.

Nomenclature

Latin symbols

C_p	Specific heat at constant pressure ($kJ\ kg^{-1}\ °C^{-1}$)
g	Gravity acceleration ($m\ s^{-2}$)
h	Specific enthalpy ($kJ\ kg^{-1}$)
Ja	Jacob number (−)
k	Thermal conductivity ($W\ m^{-1}$)
L	Length (m)
m	Mass (kg)
p	Pressure (bar)
R	Radius (m)
S	Heat exchange surface (m^2)
T	Temperature ($°C$)
u	Specific energy ($kJ\ kg^{-1}$)
U	Energy (kJ)
V	Volume (m^3)
Z	State variable vector

Greek symbols

α	Convective heat transfer coefficient ($kJ\ °C^{-1}\ m^{-2}$)
δ	Perturbation (−)
η	Input variable vector
μ	Dynamic viscosity ($Pa\ s$)
ρ	Density ($kg\ m^{-3}$)
ψ	Matrix of coefficients

Special characters

$\dot{h}$	Specific enthalpy time derivative ($kJ\ kg^{-1}s^{-1}$)
$\dot{m}$	Mass flow rate ($kg\ s^{-1}$)
$\dot{p}$	Pressure time derivative ($bar\ s^{-1}$)
$\dot{Q}$	Heat Power (kW)
$\dot{U}$	Energy time derivative ($kJ\ s^{-1}$)
$\dot{V}$	Volume time derivative (m^3s^{-1})
$\dot{z}$	State variable time derivative vector
$\dot{\rho}$	Density time derivative ($kg\ m^{-3}\ s^{-1}$)

Subscripts

FL	Flashing
RO	Rain out
SC	Superficial condensate
SP	Spray
VLV	Safety-valve
WC	Wall condensate
H	Heaters
V	Vapour
l	Liquid
G	Saturated Vapour
F	Saturated Liquid
0	Equilibrium reference state
1	Control volume 1
2	Control volume 2
2v	Vapour region of control volume 2
2l	Liquid region of control volume 2
3v	Vapour region of control volume 3
3l	Liquid region of control volume 3
vl	Vapour liquid interface
2v2l	Vapour liquid interface of control volume 2
3v3l	Vapour liquid interface of control volume 3
2l1	Control volume 2 and 1 liquid interface
3l2	Control volume 3 and 2 liquid interface
12	Control volume 1 and 2 interface
1W	Control volume 1 and pressurizer wall interface
2W	Control volume 2 and pressurizer wall interface
lW	Liquid and pressurizer wall interface
vW	Vapour and pressurizer wall interface
2vW	Vapour of control volume 2 and pressurizer wall interface
2lW	Liquid of control volume 2 and pressurizer wall interface
3vW	Vapour of control volume 3 and pressurizer wall interface
3lW	Liquid of control volume 2 and pressurizer wall interface
OUT_1	Flux exiting from control volume 1
OUT_2	Flux exiting from control volume 2
OUT_2_up	Flux exiting from control volume 2 during in-surge
OUT_2_down	Flux exiting from control volume 2 during out-surge
OUT_3	Flux exiting from control volume 3
WALL	Pressurizer wall
SAT	Saturation condition
Ext	External environment
Cond	Conductive

Acronyms

COM	Control Oriented Model
EA	Equilibrium Approach
MCV	Multiple Control Volume
NEA	Non-Equilibrium Approach
PWR	Pressurized Water Reactor
SIR	Safety Integral Reactor
SOM	Safety Oriented Model

Appendix. Pressurizer matrix formulation

TRSV sub−model STATE 1 $\boldsymbol{h_l} < \boldsymbol{h_f} \cap \boldsymbol{h_v} > \boldsymbol{h_g}$ $\dot{\boldsymbol{z}} = \{\dot{\boldsymbol{p}}, \dot{\boldsymbol{V}}_{\boldsymbol{v}}, \dot{\boldsymbol{h}}_{\boldsymbol{v}}, \dot{\boldsymbol{h}}_{\boldsymbol{l}}\}^T$

$$\psi = \begin{vmatrix} V_v * \frac{\partial \rho_v}{\partial p} & \rho_v & V_v * \frac{\partial \rho_v}{\partial h_v} & 0 \\ (V - V_v) * \frac{\partial \rho_l}{\partial p} & -\rho_l & 0 & (V - V_v) * \frac{\partial \rho_l}{\partial h_l} \\ -V_v & 0 & \rho_v * V_v & 0 \\ -(V - V_v) & 0 & 0 & \rho_l * (V - V_v) \end{vmatrix}$$

$$\eta = \begin{vmatrix} -\dot{m}_{SC} - \dot{m}_{WC} \\ \dot{m}_{SC} + \dot{m}_{INSURGE} - \dot{m}_{OUTSURGE} \\ -\dot{m}_{SC} \cdot (h_g - h_v) - \dot{Q}_{vW} - \dot{Q}_{vl} \\ \dot{m}_{SC} \cdot (h_f - h_l) + \dot{m}_{SP} \cdot (h_f - h_l) + \dot{m}_{INSURGE} \cdot (h_{INSURGE} - h_l) + \dot{Q}_H - \dot{Q}_{lW} + \dot{Q}_{vl} \end{vmatrix}$$

TRSV sub−model STATE 2 $\boldsymbol{h_L = h}$ $_f\boldsymbol{h}\varphi$ $> \boldsymbol{h}_g$ $\dot{\boldsymbol{z}} = \{\dot{\boldsymbol{p}}, \dot{\boldsymbol{V}}_{\boldsymbol{v}}, \dot{\boldsymbol{h}}_{\boldsymbol{v}}, \dot{\boldsymbol{m}}_{\boldsymbol{FL}}\}^{\boldsymbol{T}}$

$$\psi = \begin{vmatrix} V_v * \frac{\partial \rho_v}{\partial p} & \rho_v & V_v * \frac{\partial \rho_v}{\partial h_v} & 1 \\ (V - V_v) * \frac{d\rho_f}{dp} & -\rho_f & 0 & 1 \\ -V_v & 0 & -V_v & -(h_g - h_v) \\ (V - V_v) * \left(\rho_f * \frac{dh_f}{dp} - 1\right) & 0 & 0 & (h_g - h_f) \end{vmatrix}$$

$$\eta = \begin{vmatrix} -\dot{m}_{SC} - \dot{m}_{VLV} \\ \dot{m}_{SC} + \dot{m}_{SP} + \dot{m}_{INSURGE} - \dot{m}_{OUTSURGE} \\ -\dot{m}_{SC} \cdot (h_g - h_v) - \dot{Q}_{Wv} - \dot{Q}_{vl} \\ \dot{m}_{INSURGE} \cdot (h_{INSURGE} - h_f) + \dot{Q}_H - \dot{Q}_{lW} + \dot{Q}_{vl} \end{vmatrix}$$

TRSV sub−model STATE 3 $\boldsymbol{h_L < h_f \cap h_V = h_g}$ $\dot{\boldsymbol{z}} = \{\dot{\boldsymbol{p}}, \dot{\boldsymbol{V}}_{\boldsymbol{v}}, \dot{\boldsymbol{m}}_{\boldsymbol{RO}}, \dot{\boldsymbol{h}}_{\boldsymbol{l}}\}^{\boldsymbol{T}}$

$$\psi = \begin{vmatrix} V_v * \frac{d\rho_g}{dp} & \rho_g & 1 & 0 \\ (V - V_v) * \frac{\partial \rho_l}{\partial p} & -\rho_l & 1 & (V - V_v) * \frac{\partial \rho_l}{\partial h_l} \\ V_v * \left(\rho_g * \frac{dh_g}{dp} - 1\right) & 0 & (h_f - h_g) & 0 \\ -(V - V_v) & 0 & (h_l - h_g) & \rho_l * (V - V_v) \end{vmatrix}$$

$$\eta = \begin{vmatrix} -\dot{m}_{SC} - \dot{m}_{VLV} \\ \dot{m}_{SC} + \dot{m}_{SP} + \dot{m}_{INSURGE} - \dot{m}_{OUTSURGE} \\ -\dot{Q}_{vW} - \dot{Q}_{vl} \\ \dot{m}_{SC} \cdot (h_f - h_l) + \dot{m}_{SP} \cdot (h_f - h_l) + \dot{m}_{INSURGE} \cdot (h_{INSURGE} - h_l) + \dot{Q}_H - \dot{Q}_{lW} + \dot{Q}_{vl} \end{vmatrix}$$

TRSV sub−model STATE 4 $\boldsymbol{h_l = h_f \cap h_V = h_g}$ $\dot{\boldsymbol{z}} = \{\dot{\boldsymbol{p}}, \dot{\boldsymbol{V}}_{\boldsymbol{v}}, \dot{\boldsymbol{m}}_{\boldsymbol{RO}}, \dot{\boldsymbol{m}}_{\boldsymbol{FL}}\}^{\boldsymbol{T}}$

$$\psi = \begin{vmatrix} V_v * \frac{d\rho_g}{dp} & \rho_g & 1 & 1 \\ (V - V_v) * \frac{d\rho_f}{dp} & -\rho_f & 1 & 1 \\ V_v * \left(\rho_g * \frac{dh_g}{dp} - 1\right) & . & (h_f - h_g) & 0 \\ (V - V_v) * \left(\rho_f * \frac{dh_f}{dp} - 1\right) & 0 & 0 & (h_g - h_f) \end{vmatrix}$$

$$\eta = \begin{vmatrix} -\dot{m}_{SC} - \dot{m}_{VLV} \\ \dot{m}_{SC} + \dot{m}_{SP} + \dot{m}_{INSURGE} - \dot{m}_{OUTSURGE} \\ -\dot{Q}_{Wv} \\ \dot{m}_{INSURGE} \cdot (h_{INSURGE} - h_f) + \dot{Q}_H - \dot{Q}_{Wl} \end{vmatrix}$$

TRDV sub−model IN−SURGE STATE 1 $\boldsymbol{h_1 < h_f \cap h_{2l} < h_f \cap h_{2v} > h_g}$ $\dot{\boldsymbol{z}} = \{\dot{\boldsymbol{p}}, \dot{\boldsymbol{V}}_{\boldsymbol{2v}}, \dot{\boldsymbol{h}}_{\boldsymbol{2v}}, \dot{\boldsymbol{h}}_{\boldsymbol{2l}}, \dot{\boldsymbol{h}}_{\boldsymbol{1}}, \dot{\boldsymbol{m}}_{\boldsymbol{OUT,1}}\}^{\boldsymbol{T}}$

$$\psi = \begin{vmatrix} V_{2V} * \frac{\partial \rho_{2v}}{\partial p} & \rho_{2v} & V_{2v} * \frac{\partial \rho_{2v}}{\partial h_{2v}} & 0 & 0 & 0 \\ (V_2 - V_{2v}) * \frac{\partial \rho_{2l}}{\partial p} & -\rho_{2l} & 0 & (V_2 - V_{2v}) * \frac{\partial \rho_{2l}}{\partial h_{2l}} & 0 & 1 \\ V_1 * \frac{\partial \rho_1}{\partial p} & 0 & 0 & 0 & V_1 * \frac{\partial \rho_1}{\partial h_1} & 1 \\ -V_{2v} & 0 & \rho_{2v} * V_{2v} & 0 & 0 & 0 \\ -(V_2 - V_{2v}) & 0 & 0 & \rho_{2l} * (V_2 - V_{2v}) & 0 & -(h_1 - h_{2l}) \\ -V_1 & 0 & 0 & 0 & \rho_1 * V_1 & 0 \end{vmatrix}$$

$$\eta = \begin{vmatrix} -\dot{m}_{SC} - \dot{m}_{VLV} \\ \dot{m}_{SC} + \dot{m}_{SP} \\ \dot{m}_{INSURGE} \\ -\dot{m}_{SC} \cdot (h_g - h_{2v}) - \dot{Q}_{2v2l} - \dot{Q}_{2vW} \\ \dot{m}_{SC} \cdot (h_f - h_{2l}) + \dot{m}_{SP} \cdot (h_f - h_{2l}) + \dot{Q}_{2v2l} - \dot{Q}_{2l1} - \dot{Q}_{2lW} + \dot{Q}_H \\ \dot{m}_{INSURGE} (h_{INSURGE} - h_1) + \dot{Q}_{2l1} - \dot{Q}_{1W} \end{vmatrix}$$

TRDV sub−model IN−SURGE STATE 2 $\boldsymbol{h_1 < h_f \cap h_{2l} = h_f \cap h_{2v} > h_g}$ $\dot{\boldsymbol{z}} = \{\dot{\boldsymbol{p}}, \dot{\boldsymbol{V}}_{\boldsymbol{2v}}, \dot{\boldsymbol{h}}_{\boldsymbol{2v}}, \dot{\boldsymbol{m}}_{\boldsymbol{FL}}, \dot{\boldsymbol{h}}_{\boldsymbol{1}}, \dot{\boldsymbol{m}}_{\boldsymbol{OUT,1}}\}^{\boldsymbol{T}}$

$$\psi = \begin{vmatrix} V_{2v} * \frac{\partial \rho_{2v}}{\partial p} & \rho_{2v} & V_{2v} * \frac{\partial \rho_{2v}}{\partial h_{2v}} & 1 & 0 & 0 \\ (V_2 - V_{2v}) * \frac{d\rho_f}{dp} & -\rho_f & 0 & 1 & 0 & 1 \\ V_1 * \frac{\partial \rho_1}{\partial p} & 0 & 0 & 0 & V_1 * \frac{\partial \rho_1}{\partial h_1} & 1 \\ -V_{2v} & 0 & \rho_{2v} * V_{2v} & -(h_g - h_{2v}) & 0 & 0 \\ (V_2 - V_{2v}) * \left(\rho_f * \frac{dh_f}{dp} - 1\right) & 0 & 0 & (h_g - h_f) & 0 & -(h_1 - h_f) \\ -V_1 & 0 & 0 & 0 & \rho_1 * V_1 & 0 \end{vmatrix}$$

$$\eta = \begin{vmatrix} -\dot{m}_{SC} - \dot{m}_{VLV} \\ \dot{m}_{SC} + \dot{m}_{SP} \\ \dot{m}_{INSURGE} \\ -\dot{m}_{SC} \cdot (h_g - h_{2v}) - \dot{Q}_{2v2l} - \dot{Q}_{2vW} \\ \dot{Q}_{2v2l} - \dot{Q}_{2l1} - \dot{Q}_{2lW} + \dot{Q}_H \\ \dot{m}_{INSURGE} (h_{INSURGE} - h_1) + \dot{Q}_{2l1} - \dot{Q}_{1W} \end{vmatrix}$$

TRDV sub−model IN−SURGE STATE 3 $\boldsymbol{h_1 < h_f \cap h_{2l} < h_f \cap h_{2v} = h_g}$ $\dot{\boldsymbol{z}} = \{\dot{\boldsymbol{p}}, \dot{\boldsymbol{V}}_{2v}, \dot{\boldsymbol{m}}_{RO}, \dot{\boldsymbol{h}}_{2l}, \dot{\boldsymbol{h}}_1, \dot{\boldsymbol{m}}_{OUT,1}\}^T$

$$\psi = \begin{vmatrix} V_{2v} * \frac{d\rho_g}{dp} & \rho_g & 1 & 0 & 0 & 0 \\ (V_2 - V_{2v}) * \frac{\partial \rho_{2l}}{\partial p} & -\rho_{2l} & 1 & (V_2 - V_{2v}) * \frac{\partial \rho_{2l}}{\partial h_{2l}} & 0 & 1 \\ V_1 * \frac{\partial \rho_1}{\partial p} & 0 & 0 & 0 & V_1 * \frac{\partial \rho_1}{\partial h_1} & 1 \\ V_{2v} * \left(\rho_g * \frac{dh_g}{dp} - 1\right) & 0 & (h_f - h_g) & 0 & 0 & 0 \\ -(V_2 - V_{2v}) & 0 & -(h_f - h_{2l}) & \rho_{2l} * (V_2 - V_{2V}) & 0 & -(h_1 - h_{2l}) \\ -V_1 & 0 & 0 & 0 & \rho_1 * V_1 & 0 \end{vmatrix}$$

$$\eta = \begin{vmatrix} -\dot{m}_{SC} - \dot{m}_{VLV} \\ \dot{m}_{SC} + \dot{m}_{SP} \\ \dot{m}_{INSURGE} \\ -\dot{Q}_{2v2l} - \dot{Q}_{2vW} \\ \dot{m}_{SC} \cdot (h_f - h_{2l}) + \dot{m}_{SP} \cdot (h_f - h_{2l}) + \dot{Q}_{2v2l} - \dot{Q}_{2l1} - \dot{Q}_{2lW} + \dot{Q}_H \\ \dot{m}_{INSURGE} (h_{INSURGE} - h_1) + \dot{Q}_{2l1} - \dot{Q}_{1W} \end{vmatrix}$$

TRDV sub−model IN−SURGE STATE 4 $\mathbf{h_1 < h_f \cap h_{2l} = h_f \cap h_{2v} = h_g}$ $\dot{\mathbf{z}} = \{\dot{\mathbf{p}}, \dot{\mathbf{V}}_{2v}, \dot{\mathbf{m}}_{RO}, \dot{\mathbf{h}}_{2l}, \dot{\mathbf{h}}_1, \dot{\mathbf{m}}_{OUT,1}\}^T$

$$\psi = \begin{vmatrix} V_{2v} * \frac{d\rho_g}{dp} & \rho_g & 1 & 1 & 0 & 0 \\ (V_2 - V_{2v}) * \frac{d\rho_f}{dp} & -\rho_f & 1 & 1 & 0 & 1 \\ V_1 * \frac{\partial \rho_1}{\partial p} & 0 & 0 & 0 & V_1 * \frac{\partial \rho_1}{\partial h_1} & 1 \\ V_{2v} * \left(\rho_g * \frac{dh_g}{dp} - 1\right) & 0 & (h_f - h_g) & 0 & 0 & 0 \\ (V_2 - V_{2v}) * \left(\rho_f * \frac{dh_f}{dp} - 1\right) & 0 & 0 & (h_g - h_f) & 0 & -(h_1 - h_f) \\ -V_1 & 0 & 0 & 0 & \rho_1 * V_1 & 0 \end{vmatrix}$$

$$\eta = \begin{vmatrix} -\dot{m}_{SC} - \dot{m}_{VLV} \\ \dot{m}_{SC} + \dot{m}_{SP} \\ \dot{m}_{INSURGE} \\ -\dot{Q}_{2vW} \\ -\dot{Q}_{2l1} - \dot{Q}_{2lW} + \dot{Q}_H \\ \dot{m}_{INSURGE} (h_{INSURGE} - h_1) + \dot{Q}_{2l1} - \dot{Q}_{1W} \end{vmatrix}$$

TRDV sub−model OUT−SURGE STATE 1 $\boldsymbol{h_1 < h_f \cap h_{2l} < h_f \cap h_{2v} > h_g}$ $\dot{\boldsymbol{z}} = \{\dot{\boldsymbol{p}}, \dot{\boldsymbol{V}}_{2v}, \dot{\boldsymbol{h}}_{2v}, \dot{\boldsymbol{h}}_{2l}, \dot{\boldsymbol{h}}_1, \dot{\boldsymbol{m}}_{OUT,2}\}^T$

$$\psi = \begin{vmatrix} V_{2v}*\frac{\partial\rho_{2v}}{\partial p} & \rho_{2v} & V_{2v}*\frac{\partial\rho_{2v}}{\partial h_{2v}} & 0 & 0 & 0 \\ (V_2 - V_{2v})*\frac{\partial\rho_{2l}}{\partial p} & -\rho_{2l} & 0 & (V_2 - V_{2v})*\frac{\partial\rho_{2l}}{\partial h_{2l}} & 0 & 1 \\ V_1*\frac{\partial\rho_1}{\partial p} & 0 & 0 & 0 & V_1*\frac{\partial\rho_1}{\partial h_1} & 1 \\ -V_{2v} & 0 & \rho_{2v}*V_{2v} & 0 & 0 & 0 \\ -(V_2 - V_{2v}) & 0 & 0 & \rho_{2l}*(V_2 - V_{2v}) & 0 & 0 \\ -V_1 & 0 & 0 & 0 & \rho_1*V_1 & -(h_{2l} - h_1) \end{vmatrix}$$

$$\eta = \begin{vmatrix} -\dot{m}_{SC} - \dot{m}_{VLV} \\ \dot{m}_{SC} + \dot{m}_{SP} \\ -\dot{m}_{OUTSURGE} \\ -\dot{m}_{SC}\cdot(h_g - h_{2v}) - \dot{Q}_{2v2l} - \dot{Q}_{2vW} \\ \dot{m}_{SC}\cdot(h_f - h_{2l}) + \dot{m}_{SP}\cdot(h_f - h_{2l}) + \dot{Q}_{2v2l} - \dot{Q}_{2l1} - \dot{Q}_{3lW} + \dot{Q}_H \\ \dot{Q}_{2l1} - \dot{Q}_{1W} \end{vmatrix}$$

TRDV sub−model OUT−SURGE STATE 2 $\boldsymbol{h_1 < h_f \cap h_{2l} = h_f \cap h_{2v} > h_g}$ $\dot{\boldsymbol{z}} = \{\dot{\boldsymbol{p}}, \dot{\boldsymbol{V}}_{2v}, \dot{\boldsymbol{h}}_{2v}, \dot{\boldsymbol{m}}_{FL}, \dot{\boldsymbol{h}}_1, \dot{\boldsymbol{m}}_{OUT,2}\}^T$

$$\psi = \begin{vmatrix} V_{2v}*\frac{\partial\rho_{2v}}{\partial p} & \rho_{2v} & V_{vV}*\frac{\partial\rho_{2v}}{\partial h_{2v}} & 1 & 0 & 0 \\ (V_2 - V_{2v})*\frac{d\rho_f}{dp} & -\rho_f & 0 & 1 & 0 & 1 \\ V_1*\frac{\partial\rho_1}{\partial p} & 0 & 0 & 0 & V_1*\frac{\partial\rho_1}{\partial h_1} & 1 \\ -V_{2v} & 0 & \rho_{2v}*V_{2v} & -(h_g - h_{2v}) & 0 & 0 \\ (V_2 - V_{2v})*\left(\rho_F*\frac{dh_f}{dp} - 1\right) & 0 & 0 & (h_g - h_f) & 0 & 0 \\ -V_1 & 0 & 0 & \rho_1*V_1 & -(h_f - h_1) & 0 \end{vmatrix}$$

$$\eta = \begin{vmatrix} -\dot{m}_{SC} - \dot{m}_{VLV} \\ \dot{m}_{SC} + \dot{m}_{SP} \\ -\dot{m}_{OUTSURGE} \\ -\dot{m}_{SC}\cdot(h_g - h_{2v}) - \dot{Q}_{2v2l} - \dot{Q}_{2vW} \\ \dot{Q}_{2v2l} - \dot{Q}_{2l1} - \dot{Q}_{3lW} + \dot{Q}_H \\ \dot{Q}_{2l1} - \dot{Q}_{1W} \end{vmatrix}$$

TRDV sub−model OUT−SURGE STATE 3 $\boldsymbol{h_1 < h_f \cap h_{2l} < h_f \cap h_{2v} = h_g}$ $\dot{\boldsymbol{z}} = \{\dot{\boldsymbol{p}}, \dot{\boldsymbol{V}}_{2v}, \dot{\boldsymbol{m}}_{RO}, \dot{\boldsymbol{h}}_{2l}, \dot{\boldsymbol{h}}_1, \dot{\boldsymbol{m}}_{OUT,2}\}^T$

$$\Psi = \begin{vmatrix} V_{2v}*\frac{d\rho_g}{dp} & \rho_g & 1 & 0 & 0 & 0 \\ (V_2 - V_{2v})*\frac{\partial\rho_{2l}}{\partial p} & -\rho_{2l} & 1 & (V_2 - V_{2v})*\frac{\partial\rho_{2l}}{\partial h_{2l}} & 0 & 1 \\ V_1*\frac{\partial\rho_1}{\partial p} & 0 & 0 & 0 & V_1*\frac{\partial\rho_1}{\partial h_1} & 1 \\ V_{2v}*\left(\rho_g*\frac{dh_g}{dp} - 1\right) & 0 & (h_f - h_g) & 0 & 0 & 0 \\ -(V_2 - V_{2v}) & 0 & -(h_f - h_{2l}) & 0 & 0 & 0 \\ -V_1 & 0 & 0 & 0 & \rho_1*V_1 & -(h_{2l} - h_1) \end{vmatrix}$$

$$\eta = \begin{vmatrix} -\dot{m}_{SC} - \dot{m}_{VLV} \\ \dot{m}_{SC} + \dot{m}_{SP} \\ -\dot{m}_{OUTSURGE} \\ -\dot{Q}_{2v2l} - \dot{Q}_{2vW} \\ \dot{m}_{SC}\cdot(h_f - h_{2l}) + \dot{m}_{SP}\cdot(h_f - h_{2l}) + \dot{Q}_{2v2l} - \dot{Q}_{2l1} - \dot{Q}_{3lW} + \dot{Q}_H \\ \dot{Q}_{2l1} - \dot{Q}_{1W} \end{vmatrix}$$

TRDV sub−model OUT−SURGE STATE 4 $\boldsymbol{h_1 < h_f \cap h_{2l} = h_f \cap h_{2v} = h_g}$ $\dot{\boldsymbol{z}} = \{\dot{\boldsymbol{p}}, \dot{\boldsymbol{V}}_{2v}, \dot{\boldsymbol{m}}_{RO}, \dot{\boldsymbol{m}}_{FL}, \dot{\boldsymbol{h}}_1, \dot{\boldsymbol{m}}_{OUT,2}\}^T$

$$\Psi = \begin{vmatrix} V_{2v}*\frac{d\rho_g}{dp} & \rho_g & 1 & 0 & 0 & 0 \\ (V_2 - V_{2v})*\frac{d\rho_f}{dp} & -\rho_f & 1 & 0 & 0 & 1 \\ V_1*\frac{\partial\rho_1}{\partial p} & 0 & 0 & 0 & V_1*\frac{\partial\rho_1}{\partial h_1} & 1 \\ V_{2v}*\left(\rho_g*\frac{dh_g}{dp} - 1\right) & 0 & (h_f - h_g) & 0 & 0 & 0 \\ (V_2 - V_{2v})*\left(\rho_f*\frac{dh_f}{dp} - 1\right) & 0 & 0 & (h_g - h_f) & 0 & 0 \\ -V_1 & 0 & 0 & 0 & \rho_1*V_1 & -(h_f - h_1) \end{vmatrix}$$

$$\eta = \begin{vmatrix} -\dot{m}_{SC} - \dot{m}_{VLV} \\ \dot{m}_{SC} + \dot{m}_{SP} \\ -\dot{m}_{OUTSURGE} \\ -\dot{Q}_{2vW} \\ \dot{m}_{SP}\cdot(h_f - h_{2l}) - \dot{Q}_{2l1} - \dot{Q}_{3lW} + \dot{Q}_H \\ \dot{Q}_{2l1} - \dot{Q}_{1W} \end{vmatrix}$$

TRTV sub−model IN−SURGE STATE 1 $\boldsymbol{h_1 < h_f \cap h_2 < h_f \cap h_{3l} < h_f \cap h_{3v} > h_g}$ $\boldsymbol{\dot{z} = \{\dot{p}, \dot{V}_{3v}, \dot{h}_{3v}, \dot{h}_{3l}, \dot{h}_2, \dot{h}_1, \dot{m}_{OUT,2up}, \dot{m}_{OUT,1}\}^T}$

$$\Psi = \begin{vmatrix} V_{3v}*\frac{\partial\rho_{3v}}{\partial p} & \rho_{3v} & V_{3v}*\frac{\partial\rho_{3v}}{\partial h_{3v}} & 0 & 0 & 0 & 0 & 0 \\ (V_3 - V_{3v})*\frac{\partial\rho_{3l}}{\partial p} & -\rho_{3L} & 0 & (V_3 - V_{3v})*\frac{\partial\rho_{3l}}{\partial h_{lL}} & 0 & 0 & 1 & 0 \\ V_2*\frac{\partial\rho_2}{\partial p} & 0 & 0 & 0 & V_2*\frac{\partial\rho_2}{\partial h_2} & 0 & 1 & 1 \\ V_1*\frac{\partial\rho_1}{\partial p} & 0 & 0 & 0 & 0 & V_1*\frac{\partial\rho_1}{\partial h_1} & 0 & 1 \\ -V_{3v} & 0 & \rho_{3v}*V_{3v} & 0 & 0 & 0 & 0 & 0 \\ -(V_3 - V_{3v}) & 0 & 0 & \rho_{3l}*(V_3 - V_{3v}) & 0 & 0 & -(h_2 - h_{3l}) & 0 \\ -V_2 & 0 & 0 & 0 & \rho_2*V_2 & 0 & 0 & -(h_1 - h_2) \\ -V_1 & 0 & 0 & 0 & 0 & \rho_1*V_1 & 0 & 0 \end{vmatrix}$$

$$\eta = \begin{vmatrix} -\dot{m}_{SC} - \dot{m}_{VLV} \\ \dot{m}_{SC} + \dot{m}_{SP} \\ 0 \\ \dot{m}_{INSURGE} \\ -\dot{m}_{SC}\cdot(h_g - h_{3v}) - \dot{Q}_{3v3l} - \dot{Q}_{3vW} \\ \dot{m}_{SC}\cdot(h_f - h_{3l}) + \dot{m}_{SP}\cdot(h_f - h_{3l}) - \dot{Q}_{3l2} + \dot{Q}_{3v3l} - \dot{Q}_{3lW} + \dot{Q}_H \\ -\dot{Q}_{21} + \dot{Q}_{3l2} - \dot{Q}_{2W} \\ \dot{m}_{INSURGE}(h_{INSURGE} - h_1) + \dot{Q}_{21} - \dot{Q}_{1W} \end{vmatrix}$$

TRTV sub−model IN−SURGE STATE 2 $\boldsymbol{h_1 < h_f \cap h_2 < h_f \cap h_{3l} = h_f \cap h_{3v} > h_g}$ $\boldsymbol{\dot{z} = \{\dot{p}, \dot{V}_{3v}, \dot{h}_{3v}, \dot{m}_{FL}, \dot{h}_2, \dot{h}_1, \dot{m}_{OUT,2up}, \dot{m}_{OUT,1}\}^T}$

$$\Psi = \begin{vmatrix} V_{3v}*\frac{\partial\rho_{3v}}{\partial p} & \rho_{3v} & V_{3v}*\frac{\partial\rho_{3v}}{\partial h_{3v}} & 1 & 0 & 0 & 0 & 0 \\ (V_3 - V_{3v})*\frac{d\rho_f}{dp} & -\rho_f & 0 & 1 & 0 & 0 & 1 & 0 \\ V_2*\frac{\partial\rho_2}{\partial p} & 0 & 0 & 0 & V_2*\frac{\partial\rho_2}{\partial h_2} & 0 & 1 & 1 \\ V_1*\frac{\partial\rho_1}{\partial p} & 0 & 0 & 0 & 0 & V_1*\frac{\partial\rho_1}{\partial h_1} & 0 & 1 \\ -V_{3v} & 0 & \rho_{3v}*V_{3v} & -(h_g - h_{3v}) & 0 & 0 & 0 & 0 \\ (V_3 - V_{3v})*\left(\rho_f*\frac{dh_f}{dp} - 1\right) & 0 & 0 & (h_g - h_f) & 0 & 0 & -(h_2 - h_f) & 0 \\ -V_2 & 0 & 0 & 0 & \rho_2*V_2 & 0 & 0 & -(h_1 - h_2) \\ -V_2 & 0 & 0 & 0 & 0 & \rho_1*V_1 & 0 & 0 \end{vmatrix}$$

$$\eta = \begin{vmatrix} -\dot{m}_{SC} - \dot{m}_{VLV} \\ \dot{m}_{SC} + \dot{m}_{SP} \\ 0 \\ \dot{m}_{INSURGE} \\ -\dot{m}_{SC}\cdot(h_g - h_{3v}) - \dot{Q}_{3v3l} - \dot{Q}_{3vW} \\ -\dot{Q}_{3l2} + \dot{Q}_{3v3l} - \dot{Q}_{3lW} + \dot{Q}_H \\ -\dot{Q}_{21} + \dot{Q}_{3l2} - \dot{Q}_{2W} \\ \dot{m}_{INSURGE}(h_{INSURGE} - h_1) + \dot{Q}_{21} - \dot{Q}_{1W} \end{vmatrix}$$

TRTV sub−model IN−SURGE STATE 3 $\boldsymbol{h_1 < h_f \cap h_2 < h_f \cap h_{3l} < h_f \cap h_{3v} = h_g}$ $\boldsymbol{\dot{z} = \{\dot{p}, \dot{V}_{3v}, \dot{m}_{RO}, \dot{h}_{3l}, \dot{h}_2, \dot{h}_1, \dot{m}_{OUT,2,up}, \dot{m}_{OUT,1}\}^T}$

$$\Psi = \begin{vmatrix} V_{3v}*\frac{d\rho_g}{dp} & \rho_g & 1 & 0 & 0 & 0 & 0 & 0 \\ (V_3 - V_{3v})*\frac{\partial\rho_{3l}}{\partial p} & -\rho_{3l} & 0 & (V_3 - V_{3v})*\frac{\partial\rho_{3l}}{\partial h_{3l}} & 0 & 0 & 1 & 0 \\ V_2*\frac{\partial\rho_2}{\partial p} & 0 & 0 & 0 & V_2*\frac{\partial\rho_2}{\partial h_2} & 0 & 1 & 1 \\ V_1*\frac{\partial\rho_1}{\partial p} & 0 & 0 & 0 & 0 & V_1*\frac{\partial\rho_1}{\partial h_1} & 0 & 1 \\ V_{3v}*\left(\rho_g*\frac{dh_g}{dp} - 1\right) & 0 & (h_f - h_g) & 0 & 0 & 0 & 0 & 0 \\ -(V_3 - V_{3v}) & 0 & -(h_f - h_{3l}) & \rho_{3l}*(V_3 - V_{3v}) & 0 & 0 & -(h_2 - h_{3l}) & 0 \\ -V_2 & 0 & 0 & 0 & \rho_2*V_2 & 0 & 0 & -(h_1 - h_2) \\ -V_1 & 0 & 0 & 0 & 0 & \rho_1*V_1 & 0 & 0 \end{vmatrix}$$

$$\eta = \begin{vmatrix} -\dot{m}_{SC} - \dot{m}_{VLV} \\ \dot{m}_{SC} + \dot{m}_{SP} \\ 0 \\ \dot{m}_{INSURGE} \\ -\dot{Q}_{3v3l} - \dot{Q}_{3vW} \\ \dot{m}_{SC}\cdot(h_f - h_{3l}) + \dot{m}_{SP}\cdot(h_f - h_{3l}) - \dot{Q}_{3l2} + \dot{Q}_{3v3l} - \dot{Q}_{3lW} + \dot{Q}_H \\ -\dot{Q}_{21} + \dot{Q}_{3l2} - \dot{Q}_{2W} \\ \dot{m}_{INSURGE}(h_{INSURGE} - h_1) + \dot{Q}_{21} - \dot{Q}_{1W} \end{vmatrix}$$

TRTV sub−model IN−SURGE STATE 4 $\boldsymbol{h_1 < h_f \cap h_2 < h_f \cap h_{3l} = h_f \cap h_{3v} = h_g}$ $\boldsymbol{\dot{z} = \{\dot{p}, \dot{V}_{3v}, \dot{m}_{RO}, \dot{m}_{FL}, \dot{h}_2, \dot{h}_1, \dot{m}_{OUT,2,up}, \dot{m}_{OUT,1}\}^T}$

$$\Psi = \begin{vmatrix} V_{3v}*\frac{d\rho_g}{dp} & \rho_g & 1 & 1 & 0 & 0 & 0 & 0 \\ (V_3 - V_{3v})*\frac{d\rho_f}{dp} & -\rho_f & 1 & 1 & 0 & 0 & 1 & 0 \\ V_2*\frac{\partial\rho_2}{\partial p} & 0 & 0 & 0 & V_2*\frac{\partial\rho_2}{\partial h_2} & 0 & 1 & 1 \\ V_1*\frac{\partial\rho_1}{\partial p} & 0 & 0 & 0 & 0 & V_1*\frac{\partial\rho_1}{\partial h_1} & 0 & 1 \\ V_{3V}*\left(\rho_g*\frac{dh_g}{dp} - 1\right) & 0 & (h_f - h_g) & 0 & 0 & 0 & 0 & 0 \\ (V_3 - V_{3v})*\left(\rho_f*\frac{dh_f}{dp} - 1\right) & 0 & 0 & (h_g - h_f) & 0 & 0 & -(h_2 - h_f) & 0 \\ -V_2 & 0 & 0 & 0 & \rho_2*V_2 & 0 & 0 & -(h_1 - h_2) \\ -V_1 & 0 & 0 & 0 & 0 & \rho_1*V_1 & 0 & 0 \end{vmatrix}$$

$$\eta = \begin{vmatrix} -\dot{m}_{SC} - \dot{m}_{VLV} \\ -\dot{m}_{SC} - \dot{m}_{VLV} \\ 0 \\ \dot{m}_{INUSRGE} \\ -\dot{Q}_{3vW} \\ -\dot{Q}_{3l2} - \dot{Q}_{3lW} + \dot{Q}_H \\ -\dot{Q}_{21} + \dot{Q}_{3l2} - \dot{Q}_{2W} \\ \dot{m}_{INSURGE}(h_{INSURGE} - h_1) + \dot{Q}_{21} - \dot{Q}_{1W} \end{vmatrix}$$

TRTV sub−model OUT−SURGE STATE 1 $\boldsymbol{h_1 < h_f \cap h_2 < h_f \cap h_{3l} < h_f \cap h_{3v} > h_g}$ $\boldsymbol{\dot{z} = \{\dot{p}, \dot{V}_{3v}, \dot{h}_{3v}, \dot{h}_{3l}, \dot{h}_2, \dot{h}_1, \dot{m}_{OUT,2,down}, \dot{m}_{OUT,3}\}^T}$

$$\Psi = \begin{vmatrix} V_{3v}*\frac{\partial\rho_{3v}}{\partial p} & \rho_{3v} & V_{3v}*\frac{\partial\rho_{3v}}{\partial h_{3v}} & 0 & 0 & 0 & 0 & 0 \\ (V_3 - V_{3v})*\frac{\partial\rho_{3l}}{\partial p} & -\rho_{3l} & 0 & (V_3 - V_{3v})*\frac{\partial\rho_{3l}}{\partial h_{3l}} & 0 & 0 & 0 & 1 \\ V_2*\frac{\partial\rho_2}{\partial p} & 0 & 0 & 0 & V_2*\frac{\partial\rho_2}{\partial h_2} & 0 & 1 & 1 \\ V_1*\frac{\partial\rho_1}{\partial p} & 0 & 0 & 0 & 0 & V_1*\frac{\partial\rho_1}{\partial h_1} & 1 & 0 \\ -V_{3v} & 0 & \rho_{3v}*V_{3v} & 0 & 0 & 0 & 0 & 0 \\ -(V_3 - V_{3v}) & 0 & 0 & \rho_{3l}*(V_3 - V_{3v}) & 0 & 0 & 0 & 0 \\ -V_2 & 0 & 0 & 0 & \rho_2*V_2 & 0 & 0 & -(h_{3l} - h_2) \\ -V_1 & 0 & 0 & 0 & 0 & \rho_1*V_1 & -(h_2 - h_1) & 0 \end{vmatrix}$$

$$\eta = \begin{vmatrix} -\dot{m}_{SC} - \dot{m}_{VLV} \\ \dot{m}_{SC} + \dot{m}_{SP} \\ 0 \\ -\dot{m}_{OUTSURGE} \\ -\dot{m}_{SC}\cdot(h_g - h_{3v}) - \dot{Q}_{3v3l} - \dot{Q}_{3vW} \\ \dot{m}_{SC}\cdot(h_f - h_{3l}) + \dot{m}_{SP}\cdot(h_f - h_{3l}) - \dot{Q}_{3l2} + \dot{Q}_{3v3l} - \dot{Q}_{3lW} + \dot{Q}_H \\ -\dot{Q}_{21} + \dot{Q}_{3l2} - \dot{Q}_{2W} \\ \dot{Q}_{21} - \dot{Q}_{1W} \end{vmatrix}$$

TRTV sub−model OUT−SURGE STATE 2 $\boldsymbol{h_1 < h_f \cap h_2 < h_f \cap h_{3l} = h_f \cap h_{3v} > h_g}$ $\boldsymbol{\dot{z} = \{\dot{p}, \dot{V}_{3v}, \dot{h}_{3v}, \dot{m}_{FL}, \dot{h}_2, \dot{h}_1, \dot{m}_{OUT.2.down}, \dot{m}_{OUT.3}\}^T}$

$$\Psi = \begin{vmatrix} V_{3v}*\frac{\partial\rho_{3v}}{\partial p} & \rho_{3v} & V_{3v}*\frac{\partial\rho_{3v}}{\partial h_{3v}} & 1 & 0 & 0 & 0 & 0 \\ (V_3 - V_{3v})*\frac{d\rho_f}{dp} & -\rho_f & 0 & 1 & 0 & 0 & 0 & 1 \\ V_2*\frac{\partial\rho_2}{\partial p} & 0 & 0 & 0 & V_2*\frac{\partial\rho_2}{\partial h_2} & 0 & 1 & 1 \\ V_1*\frac{\partial\rho_1}{\partial p} & 0 & 0 & 0 & 0 & V_1*\frac{\partial\rho_1}{\partial h_1} & 1 & 0 \\ -V_{3v} & 0 & \rho_{3v}*V_{3v} & -(h_g - h_{3v}) & 0 & 0 & 0 & 0 \\ (V_3 - V_{3v})*\left(\rho_f*\frac{dh_f}{dp} - 1\right) & 0 & 0 & (h_g - h_f) & 0 & 0 & 0 & 0 \\ -V_2 & 0 & 0 & 0 & \rho_2*V_2 & 0 & 0 & -(h_f - h_2) \\ -V_1 & 0 & 0 & 0 & 0 & \rho_1*V_1 & -(h_2 - h_1) & 0 \end{vmatrix}$$

$$\eta = \begin{vmatrix} -\dot{m}_{SC} - \dot{m}_{VLV} \\ -\dot{m}_{SC} - \dot{m}_{VLV} \\ 0 \\ -\dot{m}_{OUTSURGE} \\ -\dot{m}_{SC}\cdot(h_g - h_{3v}) - \dot{Q}_{3v3l} - \dot{Q}_{3vW} \\ -\dot{Q}_{3l2} + \dot{Q}_{3v3l} - \dot{Q}_{3lW} + \dot{Q}_H \\ -\dot{Q}_{21} + \dot{Q}_{3l2} - \dot{Q}_{2W} \\ \dot{Q}_{21} - \dot{Q}_{1W} \end{vmatrix}$$

TRTV sub−model OUT−SURGE STATE 3 $\boldsymbol{h_1 < h_f \cap h_2 < h_f \cap h_{3l} < h_f \cap h_{3v} = h_g}$ $\boldsymbol{\dot{z} = \{\dot{p}, \dot{V}_{3V}, \dot{m}_{RO}, \dot{h}_{3L}, \dot{h}_2, \dot{h}_1, \dot{m}_{OUT.2.down}, \dot{m}_{OUT.3}\}^T}$

$$\Psi = \begin{vmatrix} V_{3v}*\frac{d\rho_g}{dp} & \rho_g & 1 & 0 & 0 & 0 & 0 & 0 \\ (V_3 - V_{3v})*\frac{\partial\rho_{3l}}{\partial p} & -\rho_{3l} & 1 & (V_3 - V_{3v})*\frac{\partial\rho_{3l}}{\partial h_{3l}} & 0 & 0 & 0 & 1 \\ V_2*\frac{\partial\rho_2}{\partial p} & 0 & 0 & 0 & V_2*\frac{\partial\rho_2}{\partial h_2} & 0 & 1 & 1 \\ V_1*\frac{\partial\rho_1}{\partial p} & 0 & 0 & 0 & 0 & V_1*\frac{\partial\rho_1}{\partial h_1} & 1 & 0 \\ V_{3v}*\left(\rho_g*\frac{dh_g}{dp} - 1\right) & 0 & (h_f - h_g) & 0 & 0 & 0 & 0 & 0 \\ -(V_3 - V_{3v}) & 0 & -(h_f - h_{3l}) & \rho_{3l}*(V_3 - V_{3v}) & 0 & 0 & 0 & 0 \\ -V_2 & 0 & 0 & 0 & \rho_2*V_2 & 0 & 0 & -(h_{3l} - h_2) \\ -V_1 & 0 & 0 & 0 & 0 & \rho_1*V_1 & -(h_2 - h_1) & 0 \end{vmatrix}$$

$$\eta = \begin{vmatrix} -\dot{m}_{SC} - \dot{m}_{VLV} \\ \dot{m}_{SC} + \dot{m}_{SP} \\ 0 \\ -\dot{m}_{OUTSURGE} \\ -\dot{Q}_{3v3l} - \dot{Q}_{3vW} \\ \dot{m}_{SC}\cdot(h_f - h_{3l}) + \dot{m}_{SP}\cdot(h_f - h_{3l}) - \dot{Q}_{3l2} + \dot{Q}_{3v3l} - \dot{Q}_{3lW} + \dot{Q}_H \\ -\dot{Q}_{21} + \dot{Q}_{3l2} - \dot{Q}_{2W} \\ \dot{Q}_{21} - \dot{Q}_{1W} \end{vmatrix}$$

TRTV sub−model OUT−SURGE STATE 4 $\boldsymbol{h_1 < h_f \cap h_2 < h_f \cap h_{3l} = h_f \cap h_{3v} = h_g}$ $\boldsymbol{\dot{z} = \{\dot{p}, \dot{V}_{3V}, \dot{m}_{RO}, \dot{m}_{FL}, \dot{h}_2, \dot{h}_1, \dot{m}_{OUT.2.down}, \dot{m}_{OUT.3}\}^T}$

$$\Psi = \begin{vmatrix} V_{3v} * \frac{d\rho_g}{dp} & \rho_g & 1 & 1 & 0 & 0 & 0 & 0 \\ (V_3 - V_{3v}) * \frac{d\rho_f}{dp} & -\rho_f & 1 & 1 & 0 & 0 & 0 & 1 \\ V_2 * \frac{\partial \rho_2}{\partial p} & 0 & 0 & 0 & V_2 * \frac{\partial \rho_2}{\partial h_2} & 0 & 1 & 1 \\ V_1 * \frac{\partial \rho_1}{\partial p} & 0 & 0 & 0 & 0 & V_1 * \frac{\partial \rho_1}{\partial h_1} & 1 & 0 \\ V_{3v} * \left(\rho_g * \frac{dh_g}{dp} - 1\right) & 0 & (h_f - h_g) & 0 & 0 & 0 & 0 & 0 \\ (V_3 - V_{3v}) * \left(\rho_f * \frac{dh_f}{dp} - 1\right) & 0 & 0 & (h_g - h_f) & 0 & 0 & 0 & 0 \\ -V_2 & 0 & 0 & 0 & \rho_2 * V_2 & 0 & 0 & -(h_f - h_2) \\ -V_1 & 0 & 0 & 0 & 0 & \rho_1 * V_1 & -(h_2 - h_1) & 0 \end{vmatrix}$$

$$\eta = \begin{vmatrix} -\dot{m}_{SC} - \dot{m}_{VLV} \\ \dot{m}_{SC} + \dot{m}_{SP} \\ 0 \\ -\dot{m}_{OUTSURGE} \\ -\dot{Q}_{3vW} \\ -\dot{Q}_{3l2} - \dot{Q}_{3lW} + \dot{Q}_H \\ -\dot{Q}_{21} + \dot{Q}_{3l2} - \dot{Q}_{2W} \\ \dot{Q}_{21} - \dot{Q}_{1W} \end{vmatrix}$$

References

Ascher, U.M., Petzold, L.R., 1998. Computer Methods for Ordinary Differential Equations and Differential Algebraic Equations. Society for Industrial and Applied Mathematics, Philadelphia, PA, USA.

Botelho, D.A., De Sampaio, P.A.B., Lapa, C.M.F., Pereira, C.M.N.A., Moreira, M., Barroso, A.C.O., 2010. The IRIS pressurizer: simulation of out-surge transients and optimization procedure to design scaled experiments. Prog. Nucl. Energy 50, 730–739.

Celata, G.P., Farello, G.E., Focardi, G., Cumo, M., 1986. Direct Contact Condensation of Superheated Vapour in Water. ENEA ISSN/0393 6325.

Gajewski, M.W., 1955. Study by Simulator Techniques of Transient Pressures in High Pressure Water Systems Utilizing a Surge Tank. Westinghouse Electric Co.

Incropera, F.P., Dewitt, D.P., 1996. Fundamental of Heat and Mass Transfer, fourth ed. John Wiley & Sons.

Kuridan, R.M., Beynon, T.D., 1998. A linearized non steady state model for the pressurizer of the safe integral reactor concept. Prog. Nucl. Energy 33, 421–438.

Nahavandi, A.N., Makkenchery, S., 1970. An improved pressurizer model with bubble rise and condensate drop dynamics. Nucl. Eng. Des. 12, 135–147.

Petzold, L.R., 1982. Differential/algebraic equations are not ODE's. SIAM J. Sci. Stat. Comput. 3 (367), 384.

Redfield, J.A., Prescop, V., Margolis, S.G., 1967. Pressurizer performance during load drop. Tests at Shippingport: analysis and test. Trans. Am. Nucl. Soc. 4, 173–181.

Sorenson, C.W., 1960. Procedure for Sizing Pressurizers for Pressurized Water Reactor. Knolls Atomic Power Laboratory.

Sungwhan, C., Jin, J., 2012. Detection and estimation of sensor drifts using Kalman filters with a demonstration on a pressurizer. Nuc. Eng. Des. 242, 389–398.

Szabo, Z., Szederkenyi, G., Gapar, P., Varga, I., Hangos, K., Bokor, J., 2010. Identification and dynamic inversion based control of a pressurizer at the Paks NPP. Contr. Eng. Pract. 18, 554–565.

Todreas, N.E., Kazimi, M.J., 1990. Nuclear Systems Volume One Thermal Hydraulics Fundamentals, first ed.ction. Taylor&Francis.

Zhang, G., Yang, H., Ye, X., Xu, H., Lu, D., Chen, W., 2012. Research on pressurizer water level control of pressurized water reactor nuclear power station. In: International Conference on Future Energy, Environment, and Materials.